МИНИСТЕРСТВО НАУКИ И ТЕХНИЧЕСКОЙ ПОЛИТИКИ РФ
ГОСУДАРСТВЕННЫЙ КОМИТЕТ РФ ПО ВЫСШЕМУ ОБРАЗОВАНИЮ

НАУЧНО-ИССЛЕДОВАТЕЛЬСКИЙ ИНСТИТУТ ПРИКЛАДНОЙ МЕХАНИКИ И ЭЛЕКТРОДИНАМИКИ МОСКОВСКОГО АВИАЦИОННОГО ИНСТИТУТА

НИИ ПМЭ

MINISTRY OF SCIENCE AND TECHNICAL POLISY OF RUSSIA
STATE COMMITTEE OF HIGH EDUCATION OF RUSSIA

RESEARCH INSTITUTE OF APPLIED MECHANICS AND ELECTRODYNAMICS OF MOSCOW AVIATION INSTITUTE

DEVELOPMENT OF HOLLOW CATHODE OF HIGH POWER MIDDLE PRESSURE ARCJET

Contract № F6170894W0744
between
EOARD and RIAME MAI

Director G.A. Popov

Principle investigator E.P. Vaulin

Technical officer V.A. Obukhov

125810, Москва, ГСП-74
Волоколамское шоссе, 4
НИИПМЭ МАИ
тел.: 158-0020
факс: 158-0367
телекс: 411746 SOKOL SU

125810, Moscow, Russia
Volokolamckoe shosse, 4
RIAME MAI
phone: (095) 158-0020
fax: (095) 158-0367
telex: 411746 SOKOL SU

REPORT DOCUMENTATION PAGE

Form Approved OMB No. 0704-0188

1. AGENCY USE ONLY (Leave blank)	2. REPORT DATE	3. REPORT TYPE AND DATES COVERED
	1995	Final Report

4. TITLE AND SUBTITLE

Development of Hollow Cathode of High Power Middle Pressure Arcjet

5. FUNDING NUMBERS

F6170894W0744

6. AUTHOR(S)

Prof. Eujeni Vaulin

7. PERFORMING ORGANIZATION NAME(S) AND ADDRESS(ES)

Moscow Aviation Institute
Volokolamskoe Shosse, 4
Moscow 125871
Russia

8. PERFORMING ORGANIZATION REPORT NUMBER

N/A

9. SPONSORING/MONITORING AGENCY NAME(S) AND ADDRESS(ES)

EOARD
PSC 802 BOX 14
FPO 09499-0200

10. SPONSORING/MONITORING AGENCY REPORT NUMBER

SPC 94-4079

11. SUPPLEMENTARY NOTES

12a. DISTRIBUTION/AVAILABILITY STATEMENT

Approved for public release; distribution is unlimited.

12b. DISTRIBUTION CODE

A

13. ABSTRACT (Maximum 200 words)

This report results from a contract tasking Moscow Aviation Institute as follows: Determine integral performances of arcjet devices in nitrogen, ammonia, and their mixtures using hollow cathode devices at low and high current levels, perform short term tests (up to 50 hours) for operational reliability and determination of capabilities.

14. SUBJECT TERMS

Nil

15. NUMBER OF PAGES

60

16. PRICE CODE

N/A

17. SECURITY CLASSIFICATION OF REPORT	18. SECURITY CLASSIFICATION OF THIS PAGE	19. SECURITY CLASSIFICATION OF ABSTRACT	20. LIMITATION OF ABSTRACT
UNCLASSIFIED	UNCLASSIFIED	UNCLASSIFIED	UL

AUTHORS AND EXECUTORS

1. E.P. Vaulin, work leader, prof.

2. V.A. Obukhov, head of the department.

3. L.V. Feoktistov, scientific worker.

4. N.V. Petukhov, designer.

WORK PARTICIPANTS

1. Y.S. Burkhanov, prof.

2. V.M. Kirillova, scientific worker.

3. M.V. Kiruyshkina, assistent.

4. O.P. Charov, engineer.

5. S.V. Margaryan, engineer.

6. V.I. Remizov, worker.

ABSTRACTS

The object of this investigation is the development of high-current hollow cathodes to be used in arcjet thrusters. This work is devoted to the design and test of hollow cathodes for arcjet thrusters at low (0.5...2 kW) and average (10...50 kW) power operating on nitrogen and nitrogen-inert gas mixtures. Two models of arcjet devices have been tested for two working parameter ranges:

1. power 0,5...1,5 kW, pressure 100-200 kPa, discharge current 10...25A, working gas - nitrogen.

2. power 10...50 kW, pressure up to 50 kPa, discharge current 200...1200 A, working gases: Ar, (Ar+He) mixture, (Ar+N) mixture.

Performances and main properties of hollow cathode erosion have been studied in the course of long-duration tests from 4 to 250 hours for different arcjet devices. Upon testing methodes of electronic microscopy have been used for diagnostics of cathode surfaces. Several significant advantages of hollow cathode arcjet devices were revealed. The work was done in terms of Contract F6170894WO744 (SPC-94-4079) between European Office of Aerospace Research and Development and Prof. Vaulin under support of RIAME MAI.

CONTENTS

INTRODUCTION

Plasma thrusters play a leading role among a great amount of gas discharge devices. The research has been conducted in the framework of Contract F6170894W0744(SPC-94-4079) under a financial support of EOARD. The experience of the scientific group of Moscow Aviation Institute headed by Prof. Vaulin gaimed in the design and research of the working process in plasma generators based on the hollow cathode arc discharge was used [1-4]. However the technical specification of the contract demanded to design and to test hollow cathodes for two new ranges of working parameters and working gases:

1) Power 0.5...2 kW, discharge chamber pressure 100...200 kPa, discharge current 10-25 A, operating gases: nitrogen, nitrogen-hydrogen-mixtures.

2) Power 10...50 kW, pressure up to 50 kPa, discharge current 200...1200 A, operating gases: nitrogen, argon, (nitrogen and Ag) and (argon and He) mixtures.

The development of plasma generator with such parameters needs to study hollow cathode physical processes under given conditions, to determine of hollow cathode basic geometry and properties, to examine hollow cathode arcjet thruster working parameters. Inspite of the fact that the research is made for the plasma arcjet thrusters results may be implemented in some devices.

As it was shown in [5...8] electrode erosion in the existing arcjet thrusters during the demanded life-time leads to noticable geometrical changes both in anode and in cathode and to efficiency decrease. Thus, the cathode lifetime problem deserves its separate examination. One of the ways to solve the lifetime problem is to develop methodes of thermal and current load dispersal in the area of the arc connecting to cathode surface. The usage of a hollow cathode is promising from this point of view because it provides a more homogenious discharge and more continuous emission zone.

Basic results of the hollow cathode arcjet discharge research at low pressures were recieved in the late 60-s and in the 70-s. We should mention the works of J.S.Delcroix, A.Brumet, A.R.Trindade, D.M.Ferreira etc. [9-13]. Fundamental research (theoretical as well as experimental) which made a valuable contribution to hollow cathode discharge problems was done by Leningrad (S.-Peterburg) scientists[14-21].

We have rather full review related to the hollow cathode arcjet research [22-26]. However, there are not many publications on the subject of operational modes and erosion rate of hollow cathodes at low and average power under pressure up to 200 kPa.

This research is dedicated to the determination of the hollow cathode arcjet integral parameters of low (to 25 A) and high (up to 1200 A) discharge current levels at average pressures.

In the first part of the paper the results of the research on hollow cathodes for arcjets in the current range of (200...1200 A) and the power value up to 50 kW for Ar, (Ar+He) mixture and (W+Ar) mixture are presented. Basic design and erosion data of W+2%La_2O_3 hollow cathode at discharge pressure up to 50 kPa are given as well. Original diagram of hollow cathode discharge start up procedure is described.

In the second part, the results of the investigation at low power (~1 kW) arcjet thruster operating on nitrogen at discharge current range of 10...25 A and discharge chamber pressure up to 200 kPa are described.

Single-cavity hollow cathodes are designed for these parametres. Cathodes were made from W+2%La_2O_3 and W+3%ThO_2. The cathode cavity diameter had two values for each material. It was revealed that hollow cathode erosion rate under the given conditions differs greatly for different materials and it depends upon the current value and its distribution along the hollow cathode surface.

In the third part of the paper, the results of the calculations of expected arcjet parameters with hollow and rod cathodes for nitrogen (N_2) and (N_2+H_2) mixture are given. Calculated results satisfactorily correspond to the experimental data.

It allows us to choose "the working point" at volt-ampere hollow cathode discharge characteristics (VAC) and to estimate the thermodynamical and electrical parameters of plasma in arc discharge channel.

ACKNOWLEDGEMENTS

The authors would like to thank Professor Magne Kristiansen, Texas Technology University, USA, for his assistance, support and invaluable suggestions. The assistance and participation of Eng. Fabrizio Scortecci, CENTROSPAZIO, Italy, is sincerely appreciated.

1. RESEARCH ON HOLLOW CATHODES IN ARC DISCHARGES.

1.1. Experimental apparatus.

Arcjet plasma generators simulating physical and thermodynamical processes in arcjet propulsion were designed for investigation of hollow cathode arc discharges. These devices should meet the following requirements:

-to provide the start up procedure, including the preheating of the cathode, firing of the preliminary discharge, initiation of the main discharge and transition to the parameters of the main discharge operational modes;

- to carry out the discharge regimes at the required pressure and power range;

- to provide the thermodynamical parameters of the output flow.

At the first stage of the research the investigation of the discharge in the power range of 10...50 kW in nitrogen, argon, Ar+He and Ar+N_2 mixtures becomes of the greatest interest.

Two models of the generators were designed and manufactured taking into accounmt the requirements mentioned above.

1.1.1. AJG-1 model.

AJG-1 model is used for investigation of the discharges at current range of 600...1200 A(power level is 50...60 kW). A schematic design of AJG-1 is shown in Fig.1.

A discharge chamber 1 has cooled walls. Cathode unit 3 and anode-nozzle 4 and accelerating nozzle 5 are mounted in the vacuum chamber. The critical cross-section of the anode-nozzle is 15 mm and the critical cross-section of the accelerating nozzle is 12 mm. The discharge chamber 1 is equipped by thermal-screens 6. The propellant is fed to the discharge chamber through the system of holes in the screens as it is shown in Fig. 1 by the arrows. For the examination of the stability and interaction of the longtitudinal magnetic field with the arc the solenoid 7 was used, creating the field with the induction 0,055 T. The anode unit consisting of the anode-nozzle and accelerating nozzle was designed to reach M=2.7.

AJG-1 was mounted in the bottom of the vacuum chamber, the schematic diagram of which is shown in Fig. 1. The windows 9 were used for optical diagnostics of plasma properties.

1.1.2. AJG-2 model.

The investigation of the discharges in the current range of 200...300 A(power 10...25 kW) with a hollow cathode was performed at AJG-2 model, shown in Fig.2. The main difference of this model from the AJG-1 is in utilising of the electrode system designed for the given power range. Anode-nozzle includes a system of rechangable elements 7,8,9. In

TEST FACILITY AND AJG SAMPLE DIAGRAM

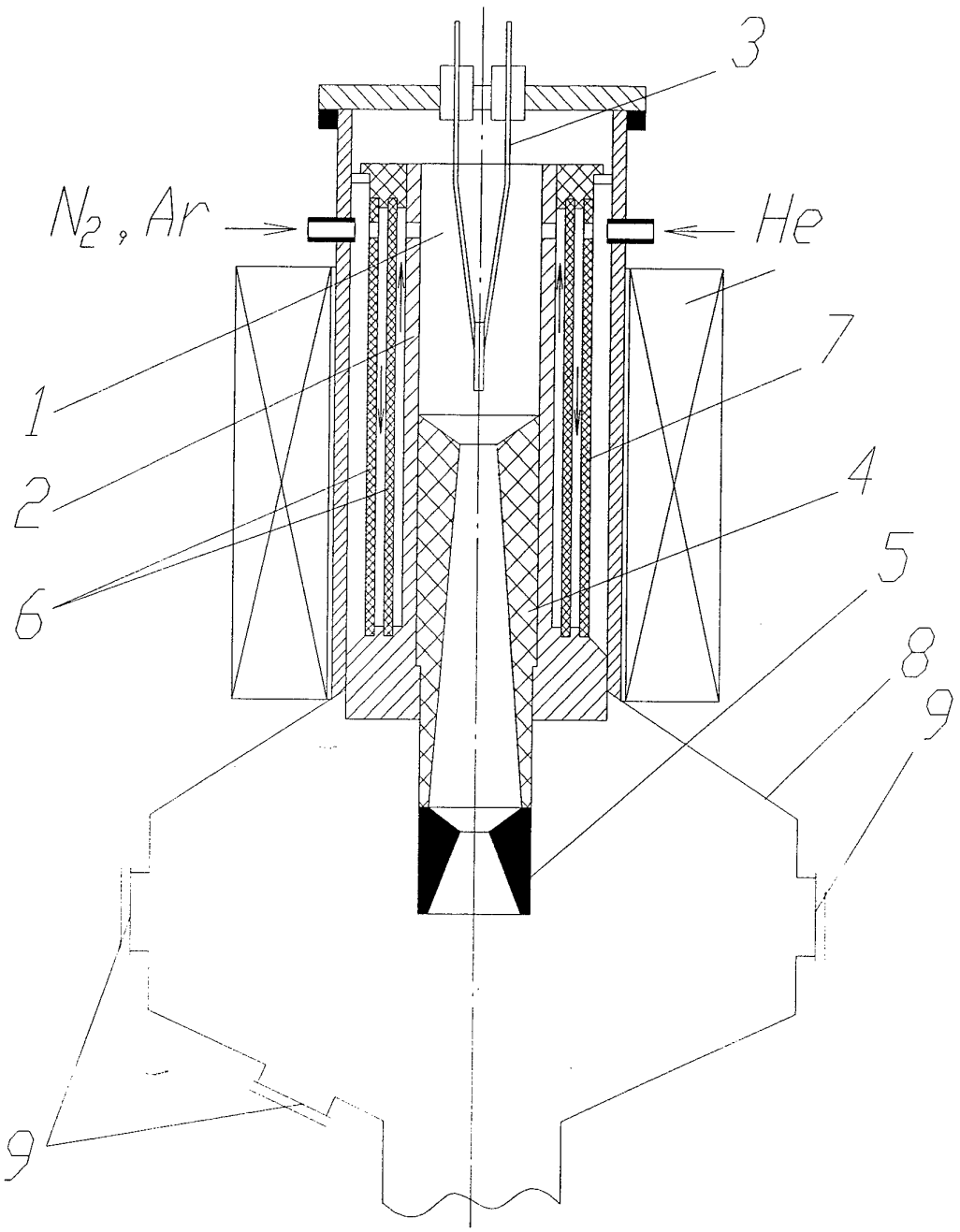

1 - discharge chamber,
2 - cooled wall,
3 - cathode assembly,
4 - anode nozzle,
5 - nozzle accelerator,
6 - heat screen,
7 - solenoid
8 - vacuum chamber flange,
9 - optical diagnostics.

Fig.1.

AJG-2 PRINCIPAL DIAGRAM

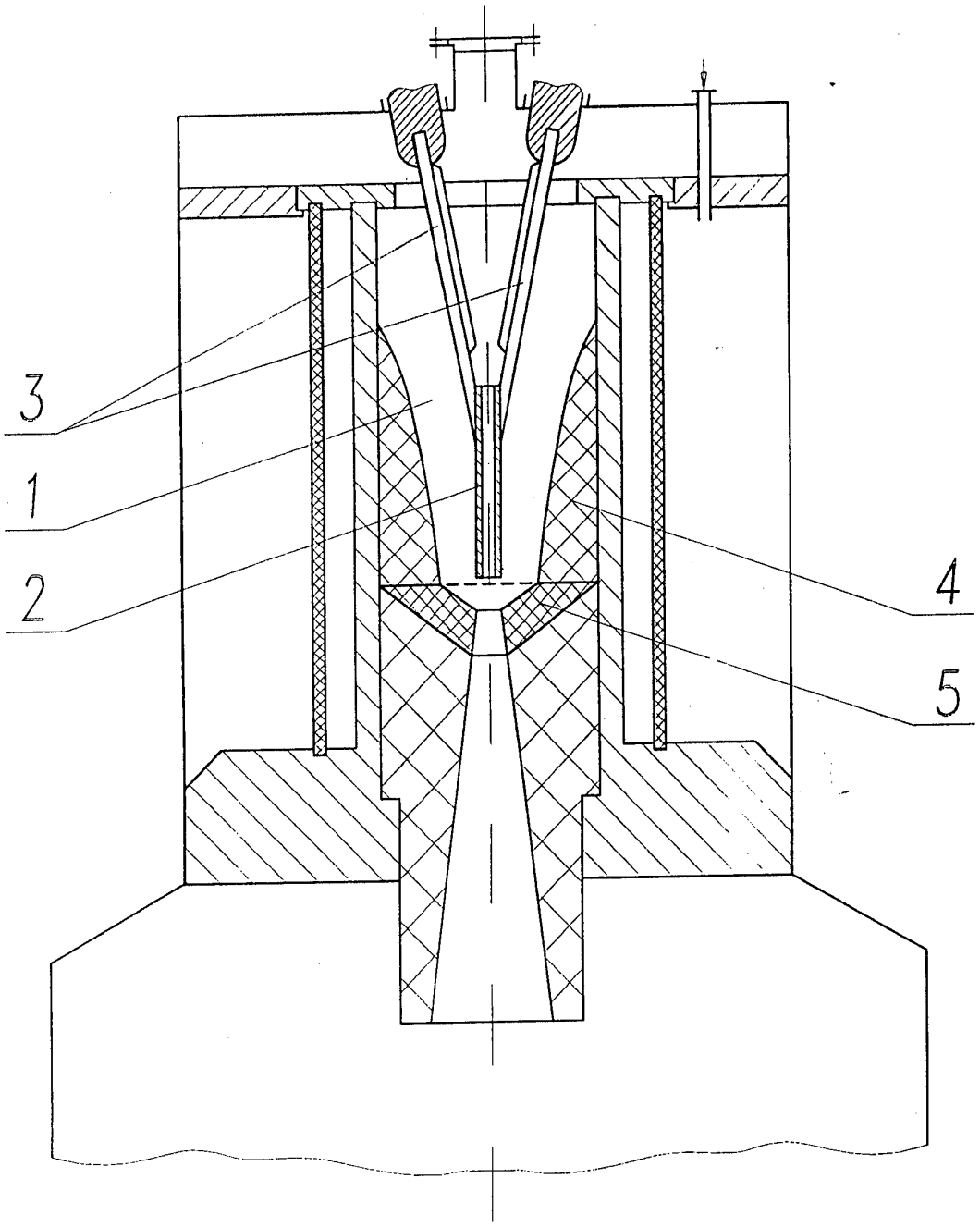

1 - discharge chamber, 3 - heated current conductors,
2 - hollow cathode, 4 - anode sections.
5 - constrictor

Fig.2.

different tests the part 8 being a constrictor had a critical cross section diameter from 3.5 to 20 mm.

1.2 Cathode unit design.

The schematic of the cathode unit design as a part of AJG-2 model is seen in Fig. 2 and is shown seperately in Fig. 3.

The cathode unit consists of a hollow cathode itself (point 2 in Fig. 2 and point 1 in Fig. 3), a system of electrical conductors (point 3 in Fig. 2 or 2,3,4 in Fig. 3).

Electrical conductors 2 (Fig.3) adjoinig the cathode have a smaller cross section than the conductors 3 (Fig. 3) and are used as emitting elements at the stage of preliminary discharge firing. The electrical conductors 3 (Fig. 3) also serve as thermal conductors for the cooling of the emitting elements by conducting of heat to the cold parts of the conductors 4 (Fig. 3). The cathode of the following design is determined as Y-like cathode unit. Taking into account the function of the conducting parts they are manufactured from different materials: emitting elements are from W+La alloys, thermal conducting parts are from W, cooling part are from W or Mo.

The design of the high current cathodes is shown in Fig.3. The cathode consists of a number of welded sticks, the amount and diameter of which are chosen due to fixed channel diameter. Only single-channel cathodes were tested in the current range of 200...1200 A. The cathode material was W+La alloy.The photo of the cathode unit is shown in Fig.4.

1.3. Experimental research of hollow cathode discharges.

1.3.1.Experimental apparatus.

The following systems were installed in the test facility consisting of:

- vacuum system including vacuum chamber 1,2 m in diameter and 2,2 m long;
- pumping system on the base of vacuum mechanical and diffusion pumps of the pumping rate up to 1500 l/s providing the residual vacuum about 10^{-3}Pa;
-system of the electric supplying including the d.c. generator 36, 200, 400 kW of electric power for the current value 300, 1000,5000 A;
- system of working gas feeding;
-system of the discharge start up;
- system of gas or water cooling;
-diagnostic systems.

1.3.2.Discharge ignition system and start up procedure.

High-current discharge firing problem (often when there is a decrease of volt-ampere characteristics) and further smooth transition of the preliminary discharge to the nominal

CATHODE ASSEMBLY DESIGN

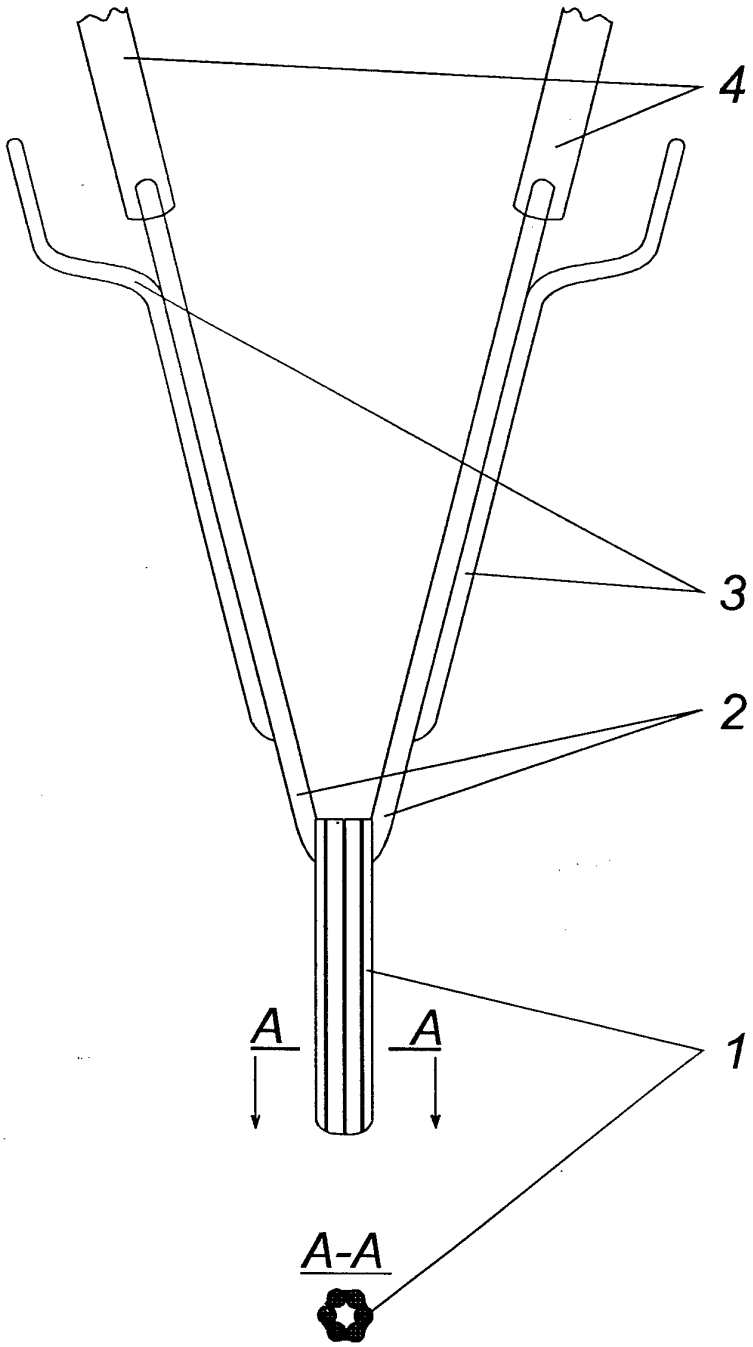

1 - singl channel hollow cathode,
2 - emitting sections of current conductors,
3 - heat conducting sections of current conductors,
4 - cooled sections of current conductors.

Fig.3.

THE PHOTO OF THE CATHODE ASSEMBLY FOR AJG-1 AND AJG-2 MODELS

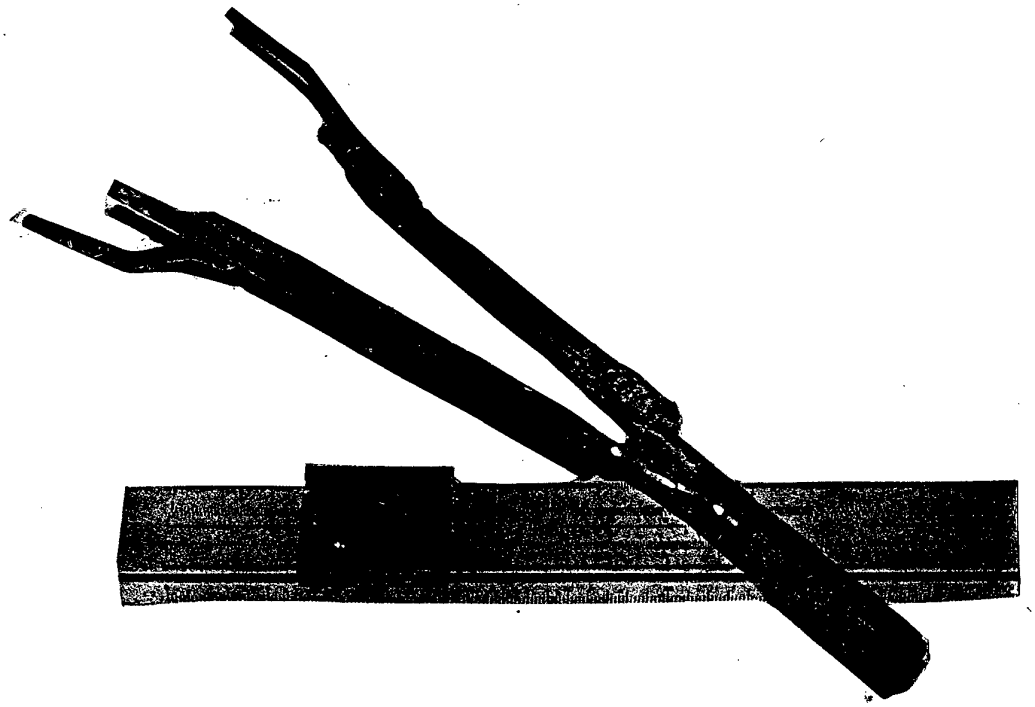

Material	$W+2\%La_2O_3$
Stics diameter	6 mm
Number of stics	5
Discarge current range	600...1200 A
Average specific erosion for Ar+He mixture	$5x10^{-12}$ кg/C

Fig.4.

operational mode always causes some technical problems. During the investigation of hollow cathode parameters which includes the determination of the average erosion rate at the nominal modes the problem of smooth start up to provide minimal erosion at the transitional regimes is of great importance.

The system of the discharge start up used in the tests is shown in Fig. 5.The same d.c. generator E is used both at the start up and at the nominal operational modes. So voltage ripples at the firing mode are minimized. Switch K_1 in "a"-position switchel on the start cathode heating circuit. The parameters of the different parts of the electrical conductors and the resistors R3 and R2 are determined to proceed the achievement of equality of the values of the anode voltages and the discharge firing voltages. The firing voltage depending upon the working gas is within 40...60 V when the emitting parts of the conductors are at the temperature corresponding to the effective emission. For example at discharge in nitrogen at pressure (1...2) 10^2 Pa and discharge current of 200...300 A the required heating current was 300...350 A and ignition voltage was 40 V. The resistance of the resistors were R_1=0.50 Ohm, R_2=0.150 Ohm,R_3=0.055 Ohm.

For argon the following parameters were obsirved: discharge current 1000...1200 A, pressure (2...3) 10^2 Pa, and discharge firing voltage 40 V. It was provided at R1=0,013 Ohm, R2=0,015 Ohm, R3=0,025 Ohm.

After discharge firing the K1-switch was turned in "b"- position and the nominal value of the discharge parametres was being achieved by the varying of the workig gas expenditure.

The parametres of the Y-cathode unit and values of R1,R2,R3 resistors could be chosen experimentally for every discharge current and gas expenditure values.

The half-empirical methode of calculation allows us also to choose the parametres of the cathode itself.

Thus, for the discharge current of 600...1200 A the cathode may consist of 5 sticks of 6 mm in diameter, made from W+La alloy.The emitting parts of the electrical conductors were made from the same alloy.

The hollow cathode for 200...300 A discharge current consisted from 6 sticks of 3 mm in diameter. The emitting elements were of the same diameter.

1.3.3. Diagnostic systems.

To measure the velocity of the directed atoms and ion in the plasma flow the temperature of the particles (atoms,electrons,ions), as well as electron density the welll-known spectral methods were used. Plasma properties in the discharge chamber were also measured. Interferometer Fabri-Pero for plasma diagnostics was used. The methodes and the results of the examination are discribed in part 1.3.5.

ELECTRIC SUPPLY DIAGRAM OF MODELS AJG-1 AND AJG-2

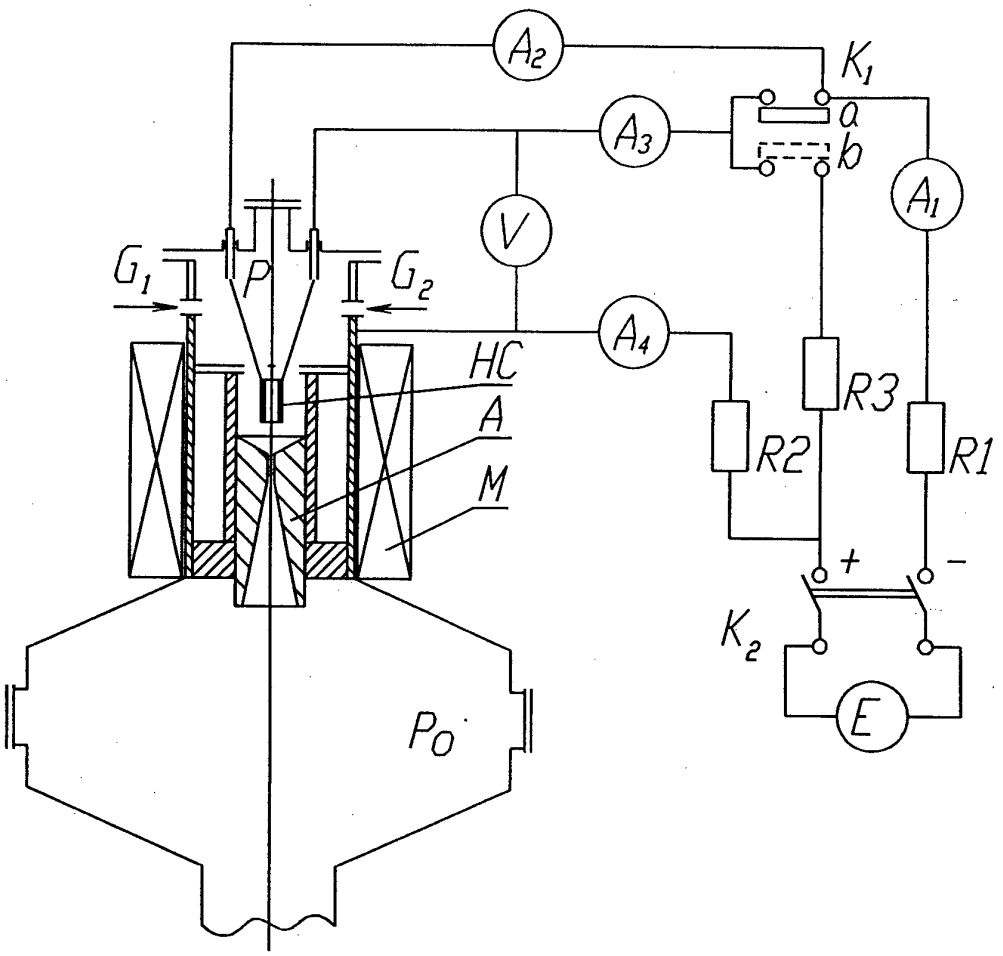

K_1, K_2 - mechanical switches,
R1, R2, R3 - resistors,
P_O - didcharge chamber
A - anode, HC - hollow cathode, M - solenoid, P - discharge chamber,
G_1, G_2 - gas feeding, E - electric supply.

Fig.5.

1.3.4. Investigation of the integral parametres of average power follow cathode AJ devices.

VAC of the discharges in different gases, under different pressures and flow rates are given in Fig.6. The investigation of the discharges at the current range of 550...1200 A was made at AJG-1, and in the range of 150...350 the AJG-2 was used.

The full working parameter range:

- flow rate m - 0.1...2.4;
- input discharge chamber pressure p=1.6...73 kPa;
- working gases: Ar (curves a and e); Ar+He (curves b,c,g); N_2 (d,h,j); Ar+N_2 (f) (Fig. 6).

The integral performances given in Fig.6 show the general conformities of the hollow cathode arc discharge inspite of the fact that different curves were obtained under different conditions and for not similar geometries of the electrode system. Thus, curves a,b,c - were obtained at the anode assembly shown in Fig. 1, curves f,g,h,j - with the electrode configuration shown in Fig. 2. In the most cases a weak magnetic field (up to 0.05 T) was used to stabilize the discharge. Dependences d and e were determined in the absence of the magnetic field. We should mention that the applying of a weak magnetic field didn't almost influence either at the hollow cathode discharge performances or at discharge stability and its azimuthal homogeneity.

That is why the magnetic field in hollow cathode are devices can not be used.

The discharge chamber gas pressure was varied by the flow rate changing and by the usage of the constrictors with different channel cross section. Thus, we could choose the discharge conditions so that at each flow rate value different pressure values could be (see for instance the curves a and e).

Average longtitudinal current density was (3...5) 10^6 A/m^2 for various regimes. Taking into account the real electrode configuration and estimating current distribution over the cathode surface we can assume that the average emission curent density changes in very narrow limits.

We can see a very low dependence of the discharge voltage on the Ar pressure and current values anording to the data of curves a and e that are shown in Fig. 6. In discharge current range of 150...1200 A the discharge voltage changes within 13.5 - 15 V. The influence of the gas kind or a percentage of gas addmixtures in Ar suchas He or N_2 is very strong. In such gas mixtures the discharge voltage and power trend to be increased. The V-A performances corresponding to the curves a,b,c, were determined at the "dynamic regime" when at the fixed gas flow "rate the electric moving force of the generator was upped meanwhile the discharge current increased from 550A to 1200 A. Then the voltage was down to lower the current in the same interval (scanning time was 7 sec). The lower current limit corresponds to the discharge extingnishing voltage. Different V-A characteristics sections are marked by the arrows at the a,b,c curves in Fig. 6. The visible small relaxation effect was caused apparently by the heat relaxations in the electrode systems.

The discharge voltage in the pure nitrogen (point j) is much higher than in Ar under the same conditions. The discharge in Ar and N_2 mixture (point f) is higher than the voltage

VOLT-AMPERE CHARACTERISTICS OF 10...50 KW AJG

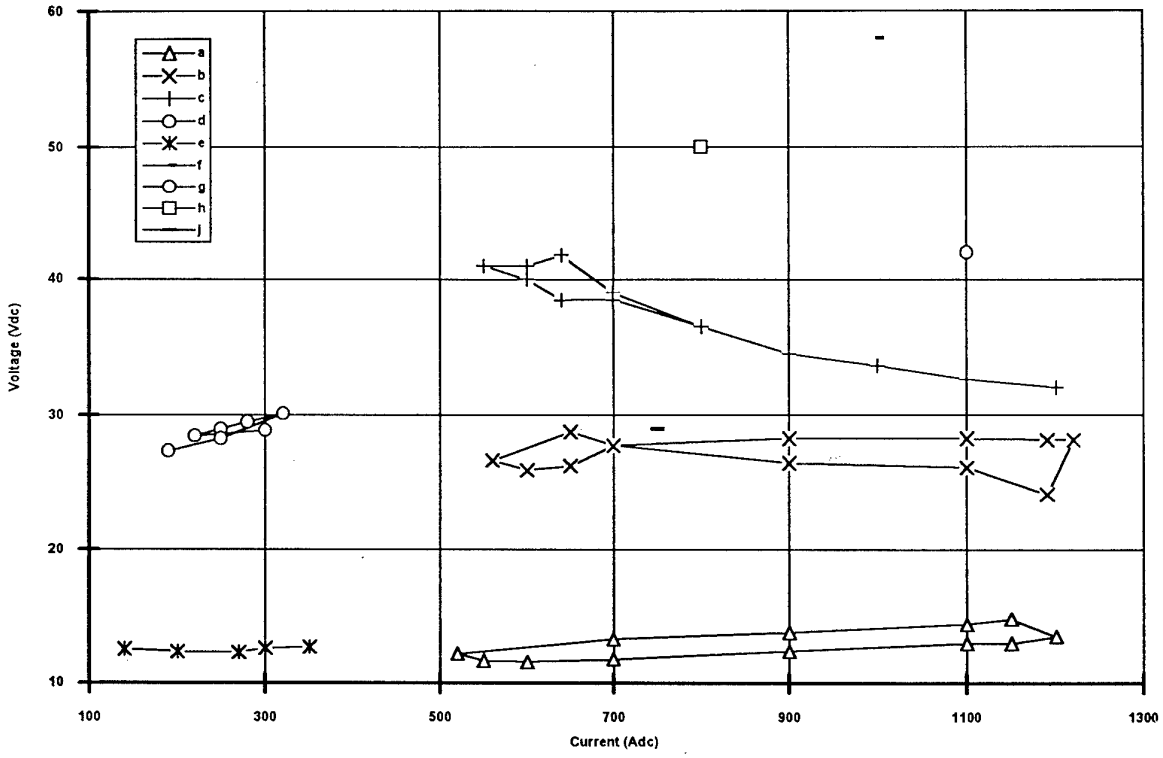

a: - Ar, p=1,6kPa, m=0,17 g/s
b: - Ar0,6+He0,3, p=7 kPa, m=0,3 g/s
c: - Ar0,4+He0,6, p=13,5 kPa, m=0,42 g/s
d: - N_2, p=20 kPa, m=0,43 g/s
e: - Ar, p=6,2 kPa, m=0,17 g/s
f: - Ar0,4+$N_2$0,6, p=40 kPa, m=0,4 g/s
g: - Ar0,75+He0,25, p=73 kPa, m=2,4 g/s
h: - N_2, p=3,8 kPa, m=0,3 g/s
j: - N_2, p=1,6 kPa, m=0,12 g/s

Fig.6.

in (Ar+He) mixture (point e). Increasing N_2 percentage in (Ar+N_2) mixture one can receive the anode temperature higher. It means that the power losses in the anode increase. Another factor, causing the growth of the discharge voltage in N_2 is evidently the energy expenditures in N_2 molecules dissociation.

Besides the marked before regularities that are typical for are discharges, we should emphasyze the special properties of the hollow cathode discharge, determining the advantages of the hollow cathodes in comparison with the stick cathodes. It mainly concerns the high azimuthal homogenity of the positive plasma colomn and of the current distribution over the anode surface consequently. This property was observered in the whole range of the tested discharge conditions and for all electrode system geometries.

This conclusion is confirmed by the photos of the anode parts that are shown in Fig. 7. They are taken from the side of the discharge chamber. Anode "a" with the constrictor diameter of 10 mm was used in Ar-discharge with the stick cathode influenced by an axial magnetic field at the discharge current value of 700 A and pressure 10 kPa.

The azimuthal heterogencity of the current distribution over the anode surface is clearly displayed in the photo.

Anode "b" with the cosstrictor diametre of 20 mm was used with the hollow cathode (work time 10 hours) at the current value of 1200 A. The working gas was (Ar+He) mixture pressure - 1,6 kPa.

Anode "c" corresponds with the following condition: working gas - (Ar+He), current power is 1500 A, constrictor diametre is 30 mm. The inner surface of the anode b after 0,5-hour tests at current value 1000 A in the (Ar+N_2) blend nuch the pressure of 40 kPa is pichured in Fig. 7. As we can realize from the deterioration type a great azimuthal homogenity and axial symmetry of the current distribution over the anode surface takes place (Fig. 7, b,c,d).

The longitudial section of the cathode after the 17-hour endurance test is shown in Fig. 8 to analyze the whole picture.

From the cathode form changing one can conclude that discharge current closes both on the inner and on the outer surfaces of the cathode. A good axial symmetry of the cathode erosion is also visible. Average specific cathode errosion was $5x10^{-12}$ kg/c.

1.3.5. Determination of plasma flow performance.

1.3.5.1. Determination of plasma flow directed movement.

The velocity of the directed atom and ion movement in a flow was determined by the Doppler's spectrum line shift. Spectra were detected with the help of Fabri-Perot interferometer fastened to the ISP- 51 spectrograph (Russia). The pictures of the interferencial friuges that were observed cross and along the flow were taken one after another by turning of the spectrograph's prysms a bit. The measurements were made using the lines Arl, ArI, HeI. The results of the measurments of dependence on gas flow rate are

VIEW OF THE WORKING ANODE SECTIONS OF AJG-1 AND AJG-2 MODEL

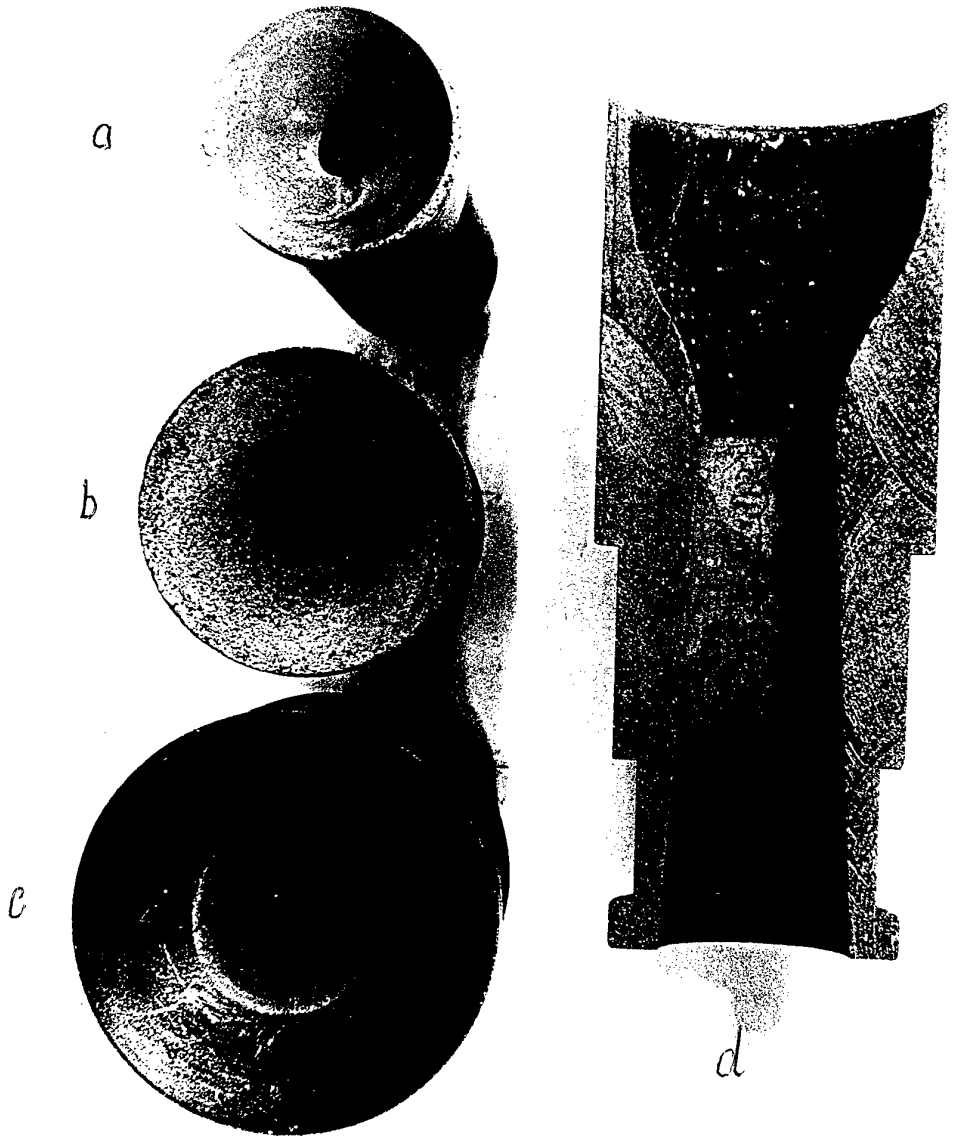

discharge chamber view

a - constrictor diameter 10 mm, Ar+He, P=10 кPa, stick cathode

b - constrictor diameter 20 mm, Ar+He, P=1,6 кPa, discarge current 1200 A,

c - constrictor diameter 30 mm, Ar+He, P=1,6 кPa, discarge current 1500 A,

side view

d - anode b, Ar+N_2, P=40 кPa, discharge current 1000 A

Fig.7.

VIEW OF HOLLOW CATHODE CHANNEL AFTER 17-HOUR TESTS IN ARGON

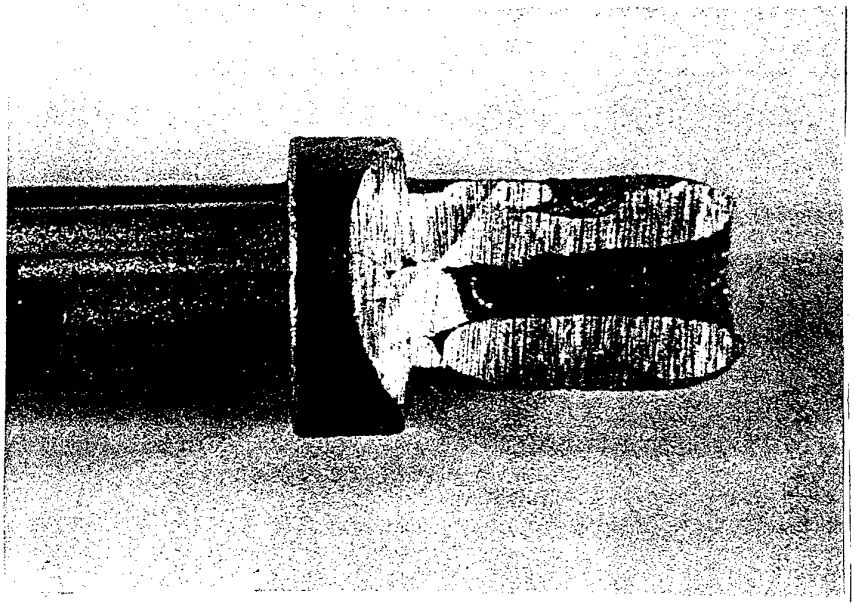

Material	$W+2\%La_2O_3$
Number of stics	6
Stick diameter	3 mm
Discharge current	200...400 A
Average specific erosion	$5x10^{-12}$ кg/C

Fig.8.

given in Fig. 9. Ar and (Ar+He) working gases are compared. The Ar-He flow velocity grows with the increase of He flow rate from 4000 to 6000 m/sec. The Ar flow velocity increases a little at first with the flow rate going up then becomes constant 2500 m/sec.

1.3.5.2. Determination of plasma flow component temperature.

The gas temperature was determined by the Doppler expaunsion with of the spectrum lines ArI (4200, 4300 A), ArII (4806 A) and HeI (5015 A). The estimation of the Reynolds criteria shows that the investigated flows are laminar (Re<800) and the used method is acceptable. The measurements of the contours were done by Fabri-Perot interferometer equipped with photoelectric reqistrator. The influence of the interferometer apparatus functions were taken into consideration. The lines with low values of Stark effect constants were chosen for measurements. The temperature data determined on ArI, ArII, HeI lines for different gas flow rates are given in the table. It is apparent that gas temperature doesn't depend upon the flow rate and structure of the flow. The excitation temperature was determined by the method of relative intensities of ArI lines belonged to the transition groups 4s-5p and 4p-5d (wave lengths within 4198-5606A). The values of transition probability were taken from [27,28]. The selfabsorbtion of the lines under the test conditions may be ignored. The flow spectrum was photographed by the ISP-51 spectrograph with the chamber focus length f=270 mm. The heterochromo -photometry method was utilised with the lamp CU-16 (Russia) as a standard light source. The dependence of lg I on exciation energy of the upper level E is shown in Fig. 10. There I - line intensity (rel.units); g - upper level statistic weight; A - transition probability.

The data corresponds to the (Ar-He) flow at the flow rate m_{He}=0,62 g/s, m_{Ar}=0,17 g/s. The straight line of the plot shows quasibolizman distribution of upper energetic levels. The inclination of the line corresponds to excitation temperature Tex=4000 K. The received values of Tex for the flows with different Ar and He flow ratio are shown in the table. The estimated relative error of the measurements is +10%. As one can see from the table Tex doesn't depend on gas flow rate though its value is higher for pure Ar flow than for (Ar+He) mixture. This difference can be explained by slow rate of electron temperature relaxation in pure Ar (due to the difference between the atomic masses of Ar and He). Comparing the excitation temperature with the temperature of heavy particles one can conclude that there is equilibrium in the gas flow under the above mentioned conditions.

The measurements of the gas temperature and the excitation temperature were made also inside the discharge chamber. The observations were made through an optical window located in the upper part of the chamber. We could observe only a small discharge area near the anode because of the design peculiarities of the device. The heavy particles temperature in (Ar+He) flow was determined with the usage of the lines ArII (4806 and 4348 Ao) at the flow rate mHe=0,62, mAr=0,17. The excitation temperature at this mode was determined using the lines of ArII group.

DEPENDENCE OF DIRECTED GAS VELOCITY ON GAS FLOW RATE

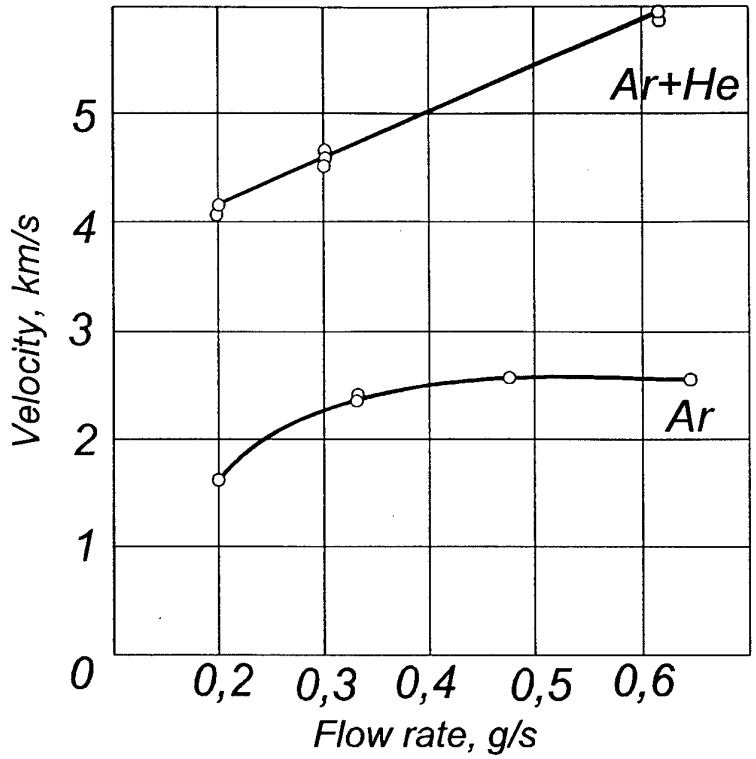

Fig.9.

DEPENDENCE OF VALUE $\lg\frac{I\lambda}{gA}$ ON EXITATION ENERGY OF UPPER ENERGETIC LEVEL E, CM^{-1}

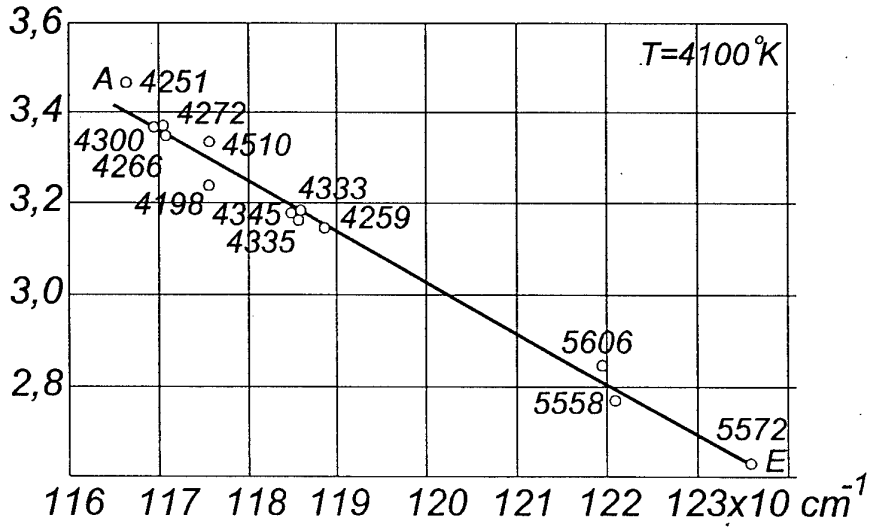

Fig.10.

			Argon flow					(Ar + He) flow	
Flow rate, g/s	0,20	0,33	0,46	0,65	He* flow rate, g/s	0,12	0,20	0,30	0,62
T_g, K	1000	1900	1800	1800	T_g, K	1700	2000	1800	1900
T_{ex}, K	4700	5000	4900	4700	T_{ex}, K	4200	4100	4300	4100
*Argon flow rate is equal 0,17 g/s									

With the accuracy of the measurements the temperatures were similar and equal to 13000 K. It shows that, probably, the thermal equilibrium condition exists in the discharge chamber at the given gas flow rate. "The break" of the electrone and heavy particle (atoms and ions) temperatures in the flow appears while the plasma expanding process in the nozzle due to the great difference between their specific heat capacities [29]. The estimations of the relaxation time τ_{rel} of the electron temperature due to atom and ion elastic collision energy exchange shown that its value is comparable with the time τ_f of the flowing of the gas through the nozzle. Thus, for Ar $\tau_{rel} > \tau_f$ but for (Ar+He) $\tau_{rel} < \tau_f$. That is why Tex is never equal to gas temperature Tg. Maybe the processes leading to the electron heating such as three-particle recomenbination and electron-metastable atom collisions are important for this effect [30,31].

1.3.5.3. Determination of electron concentration in plasma flow.

The Fabri-Perot interferometer of the millimeter range was used to determine the electron concentration in the range of $2x10^{11}$ - $6x10^{12}$ cm^{-3}. For higher electron densities the method of Stark expansion was used (for H_β line).

The schematic of the device is shown in Fig. 11. Clistron generator signal (λ =8 mm) coming through the horn and focusing lens reaches the interferometer made by two reflectors. The reflectors are the concave metal plates with the holes. The tested plasma flow is located in the interferometre centre. Then the the signal is directed by the lenses and horn to the crystal detector and registered by an oscilograph. The membrane serves to supress the high frequency vibrations in the interferometer. The usage of spherical mirrors and focusing lenses allows at the proper choice of the mirror curvature to gain the best focussing of the probe field in the centre of the interferometer.

In the absence of plasma the system was preliminary fixed in the resonance by moving of one of the mirrors. When plasma begins to flow the resonance maximum will be observed at the other resonator length. Phase drift $\Delta\alpha$, caused by the plasma was determined by the resonator length changing (Δ L) which is connected with the electron concentration n_e and flow diameter d by the ratio: $n_e = \frac{m_e c^2 \Delta\alpha}{e^2 \lambda d}$

MEASUREMENT OF ELECTRON DENCITY BY SHF FABRI-PERO INTERFEROMETER

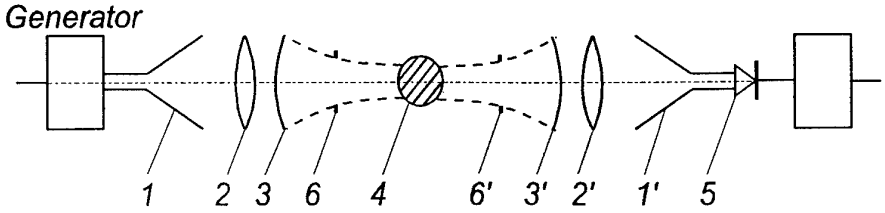

1, 1' - sending and recording horns; 2,2' - focusing lenses 3, 3' - resonators; 4 - plasma plume; 5 - detector; 6, 6' - diafragms.

Fig.11.

DEPENDENCE OF ELECTRON DENCITY ON AR FLOW RATE

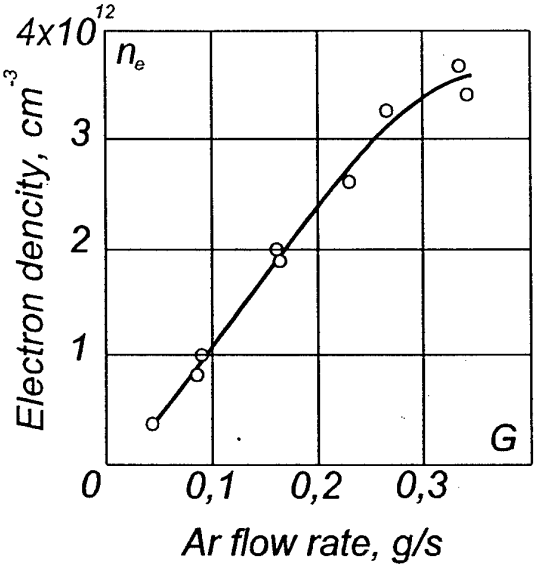

Fig.12.

DEPENDENCE OF ELECTRON DENCITY N_E ON AR+HE FLOW RATE

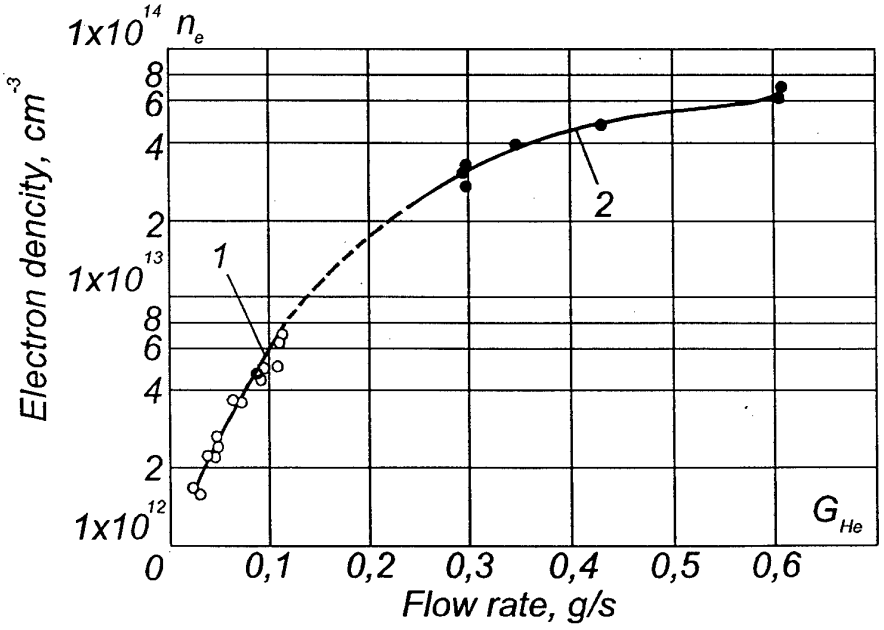

Fig.13

The results of measurements of the electron density in Ar flow depending upon the flow rate are shown in Fig. 12. The n_e value corresponds to the average mean of flow diameter. The dependence of n_e on He flow rate in (Ar+He) flow is plotted in Fig. 12. The accuracy of ne measurments estimated by the reproducing of the results of some measurements is 15%. The described method was utilised only in the measurements at low He consumptions (curve 1 in Fig. 13).

The measurements in the flow of higher density were made by the method of Stark expansion of H_β line. Small portion of H_2, approximately 1% of particle amount, was fed into the flow. The contours of H_β lines were registred with the help of Fabri-Perot interferometre equiped by ISP-51 spectrograph and photoelectric device FIP-1 (Russia). Electron density calculation on H_β line was made according to [32]. The account of the distortions due to Dopler expansion and apparatus width was made by the method described in [33]. Stark profiles of H_β line were approximated by the Foight functions. The results recieved for Ar-He flow are plotted in Fig. 13 (curve 2). As one can see from the plot the dependences received with the help of super high frequency interferometer and by the optical method are easily correlated. It's evident that the results of both method are coordinative. The measured electron density of the flow is much higher than the equilibrium value (calculated for Te=4000 K). It's evident that in the flow exhausing in vacuum there is observed the effect of n_e "frozen". Theoretical interpretation of this effect is discussed in [2].

1.3.6. Basic AJG thermodynamic and thruster performances.

The dependences of main thermodynamic and thruster parameter of arcjet devices with hollow cathode are given in Fig. 14. We should emphasize, that the main goal of this research was to examine the properties of hollow cathode high current arc discharges. The questions of the accelerating channel optimization (system:anode - nozzle) were out of this research field. Inspite of that the gained results consist a lot of useful imformation about the thermodynamic and plasmodynamic processes in the hollow cathode arc generators.

The device shown in Fig. 1 was used in the most of tests. The mixture of Ar+He with different percentage of He was used as a working gas. The discharge current was kept constant (~1200 A) for the whole range of parameters given in Fig. 14.

In flow rate range 0,17...0,8 g/s the device parameters were being changed in the following limits:

- the discharge power N=15...60 kW;
- working gas molar mass: M=4.0...5.2 Kmol;
- specific impulse: Isp=(1,5...6) 10^3 m/s;
- total specific enthalpy: Hoo=10...30 MJ/kg;
- static flow temperature: Tst=1900...2200 K;
- discharge chamber pressure: P=1.6...21 kPa;
- total efficiency: η_t =6.5...29%.

THERMODYNAMICAL PROPERTIES OF AJG-1 MODEL

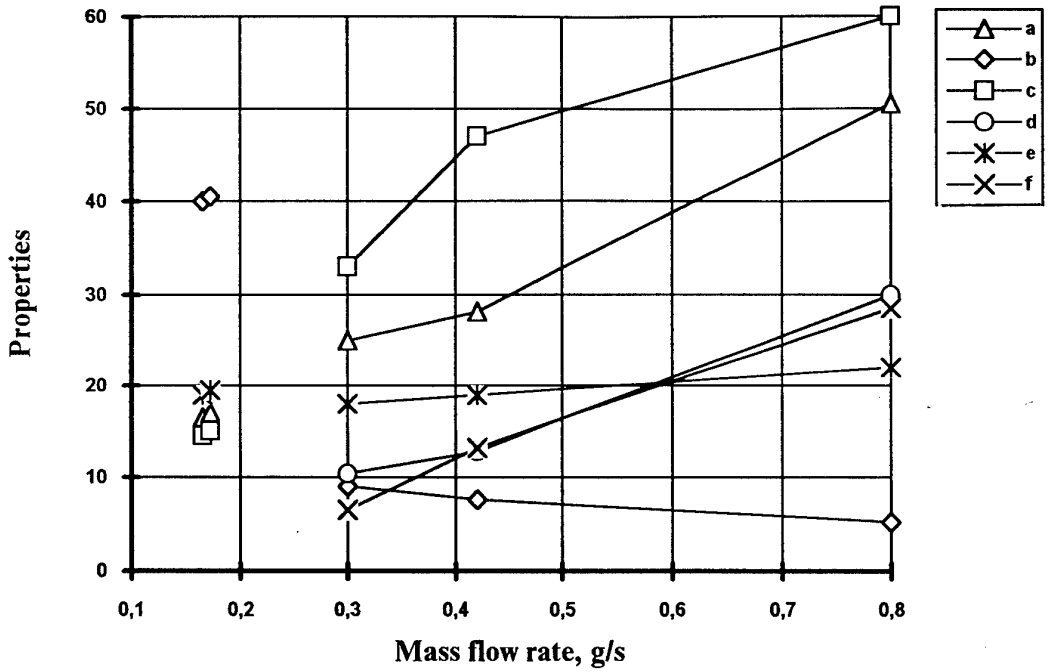

On Y-axis

Single points - Ar+He

Double points - Ar

a - Nd - discharge power, kW

b - M - molar mass of gas mixture , kmol

c - $I_{sp}x10^{-2}$ - specific impulse, m/s

d - H_{oo} - specific entalpy, MJ/kg

e - $T_{st}x10^{-2}$ - static temperature

f - η_T - thruster efficiency

Fig.14.

We can conclude from the data given above that the power, specific impulse and enthalpy grow with the increasing of the He percentage in the mixture. We should observe the same tendency using hydrogen-containing gases.

2. RESEARCH AND DEVELOPMENT OF THE LOW-POWER HOLLOW CATHODE ARCJET DEVICES.

2.1. Low power AJT experimental model.

2.1.1. General design.

Low-power AJT model was designed taking into account the following requirements:
- to provide the start up procedure, including discharge firing and transition to the nominal operational mode;
- to reach operational parameters in the given range: discharge current 10...25 A; gas pressure 100...200 kPa;
- to provide the discharge stability and homogenity.

The anode channel configuration of the 1 kW AGT was accepted as a prototype designed by CENTROSPASIO (Pisa, Italy) and described in [9,10]. The schematic of the hollow cathode AJT is given in Fig. 15.

The main design units are: 1 - ingector (material W); 2 - anode (W); 3,10 - insolator (Bornitrid); 4,5,6,7,8,30,31,32 - parts of connecting unit; 9 - housing; 11,23,24,25,26,27,28,29 - parts of cooled unit of anode electric supply; 12 - output insulator ; 13 - compacting blanket; 14,15,16,17,18,19 - cathode unit parts; 20 - hollow cathode (W; W+La: W+Th); 21,22 - AJT assembly parts. Dimentions are shown in the drawing.

The parts of the anode unit are described in [10]. The hole diameter of the constrictor is - 0.6 mm. The photo of the experimental model is shown in Fig. 16.

The AGT joined the device for the hollow cathode position control providing the placement precision of 0.01 mm is given in Fig. 17.

The thruster model with the flange and current conductors is shown in Fig. 18. The high current electric feld throughs are well seen in the Fig. 18.

The mounting flange is installed on the vacuum chamber top that schematically is shown in Fig. 15.

2.1.2. Hollow cathode unit design.

The cathode configuration designed for the current value of 10...25 A is given in Fig. 19. The hollow cathode is a rod of 3 mm in diameter with a cavity of 12 mm deep drilled at the working tip.

1 KW ARCJET ASSEMBLY

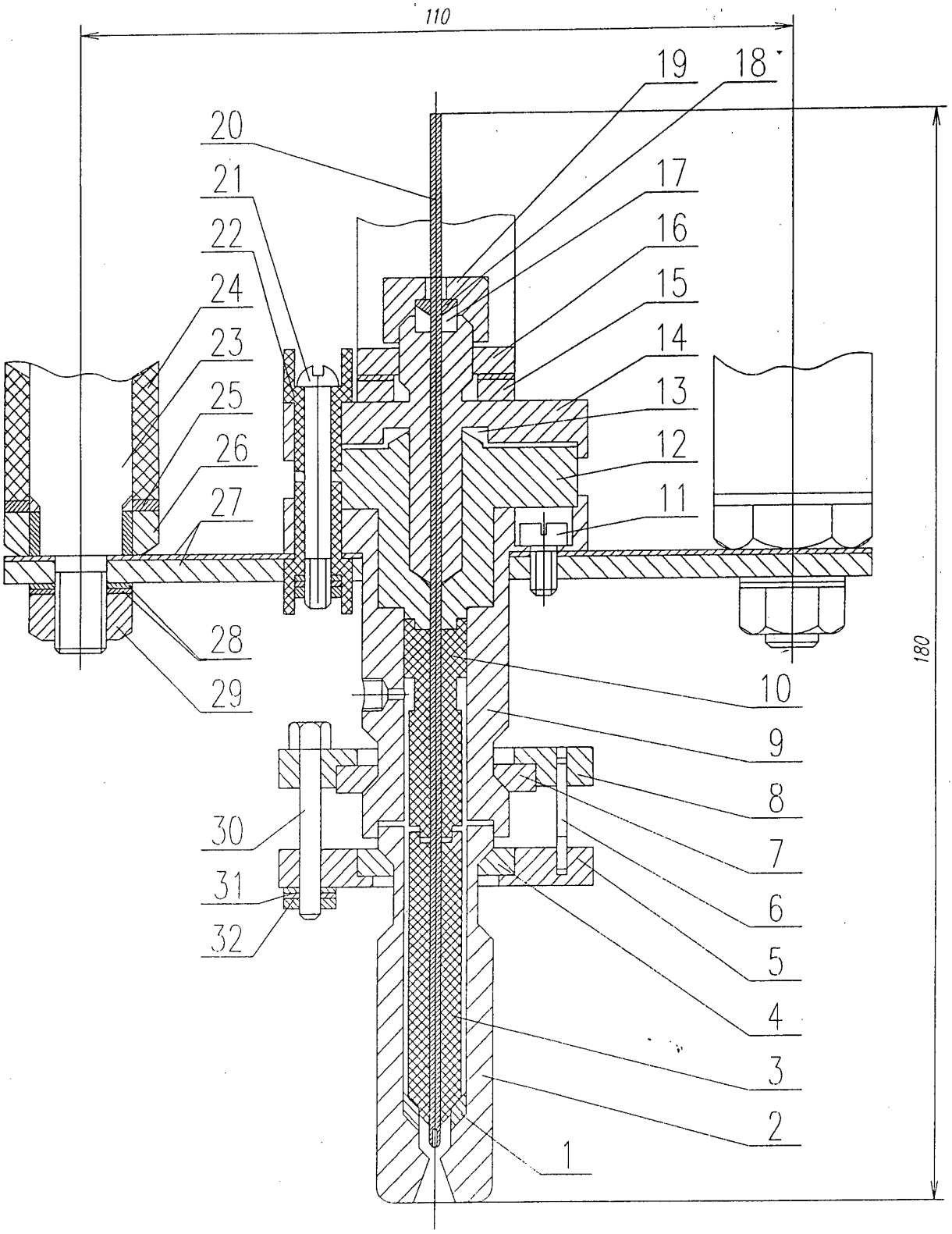

Fig. 15.

1 KW ARCJET DEVICE

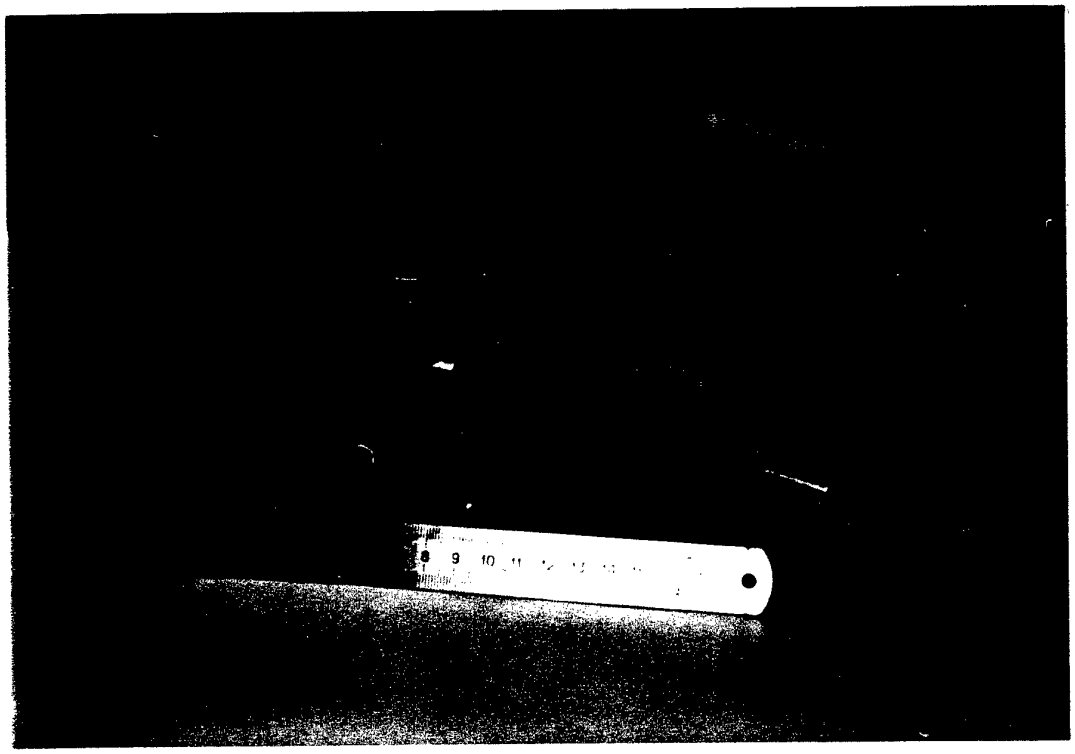

Fig. 16.

1 KW ARCJET WITH CATHODE SHIFTER

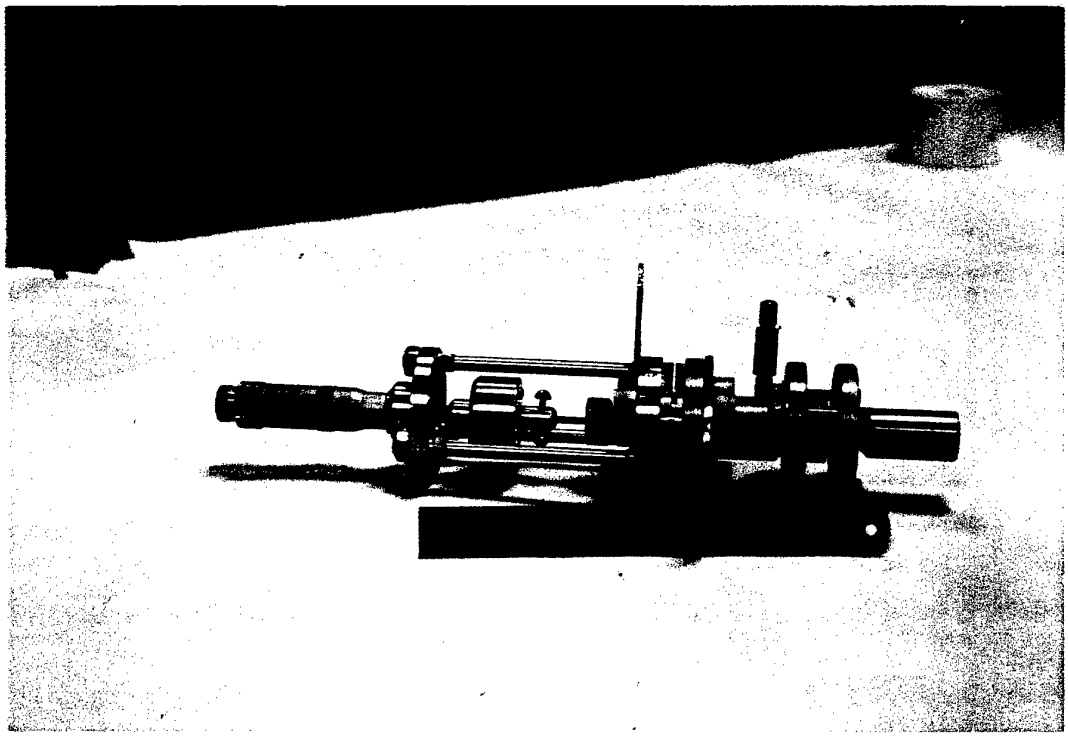

Fig. 17.

1 KW ARCJET ASSEMBLY

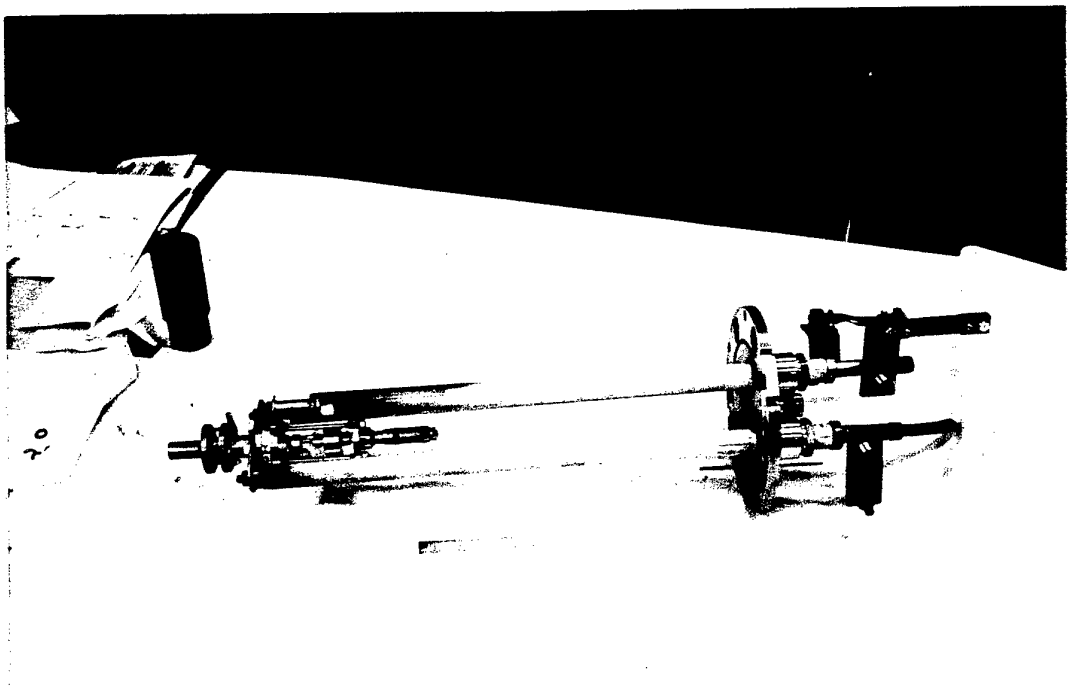

Fig. 18.

1 KW ARCJET HOLLOW CATHODE DESIGN

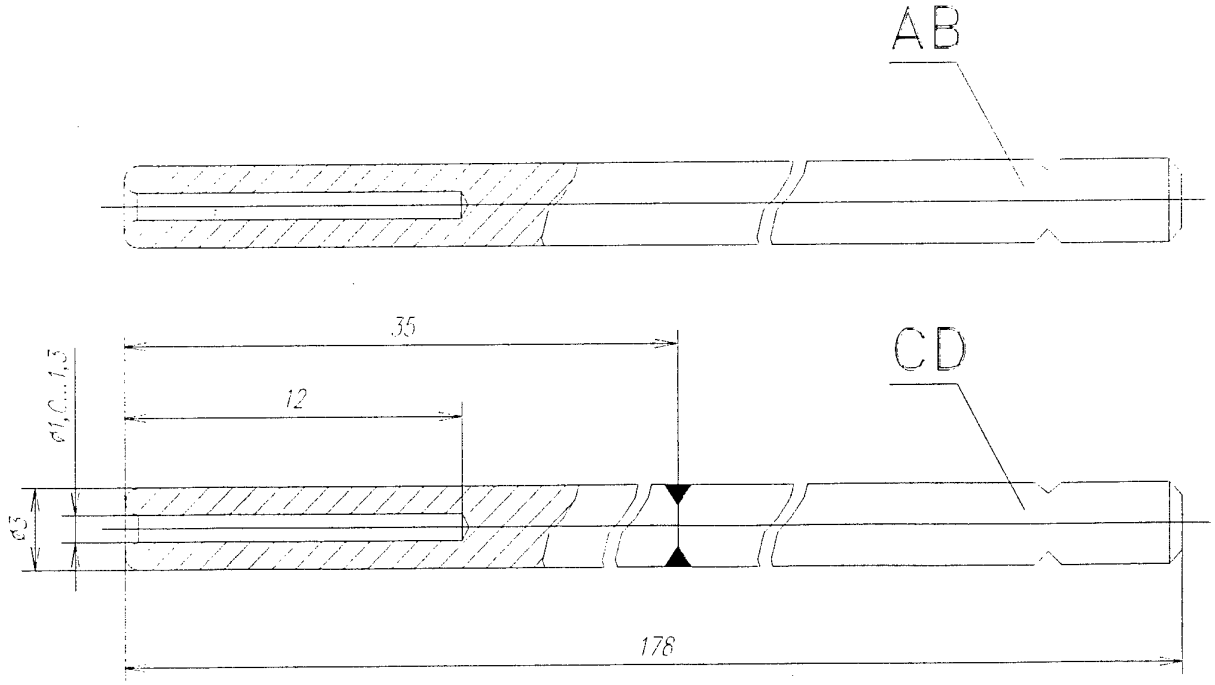

A, B - Tungsten + 2% La_2O_3
C, D - Tungsten + 3% ThO_2

A, C - cavity diameter 1 mm
B, D - cavity diameter 1,3 mm

Fig. 19.

The cavity diameter was varied from 1 to 3 mm. W+2%La_2O_3 cathodes A,B (polycrystal structure) manufactured from the whole rod. The W+3%ThO_2 cathodes C,D (polycrystal structure) 35 mm long has a working part welded to the W rod. The working cathode tip is mashined to achive round edges as it is shown in Fig. 19.

Two variants of the cathode placing in the discharge chamber were tested as it is shown in Fig. 20,21. The difference of the insulator's form and dimensions is seen. In all tests the same anode was used, the schematic of which is given in Fig. 21. In the first version of the design the insulator was similar to the insulator that has been used in [10,11]. As the tests have shown the insulator errosion was intolerably high in this design. To decrease the erosion rate another modification of the device was designed (Fig. 21), which bahavour in the tests was acceptable. The optimization of the discharge chamber configuration is the main goal of further investigation.

2.2. Results of experimental research.

2.2.1. Experimental apparatus.

The tests were made at the test facility described in part 1.3.1. The AJT was placed in a vacuum chamber as it is schematically shown in Fig. 22. Discharge initiations were made with the help of the plasma source D mounted at the thruster exit (Fig. 22). The electric feeding diagram is given in Fig. 22. The resistance of the water-cooled resistors R_1=0,225 Ohm; R_2=0,825 Ohm were choosen experimentally and used for measuring of the discharge current ripples. The resistor R_3=0...6,5 Ohm is a load.

2.2.2. Starting up procedure.

The discharge initiation is made due to creating of the plasmoid at the output thruster cross-section. The high-voltage (1500 V) and low-current (0,5 A) arc generator not electrically connected with the thruster electrode system was used for this purpose.

The firing voltage of the main discharge was set at the thruster electrodes from the main generator so that the current value in the main discharge does not exceed 25 A after the discharge firing.

At the operation in N_2 the firing voltage was 140...150 V, resistance of R_3=6,5 Ohm, discharge chamber pressure 5 kPa and vacuum chamber pressure 25 Pa. After the discharge firing the operational mode of the discharge was achived by the increas of the gas flow rate.

Operational mode parameters were following:

- pressure 100...200 kPa;
- voltage 55...65 V;
- current 10...20 A.

1 KW HOLLOW CATHODE ARCJET CONFIGURATION

(1-st modification)

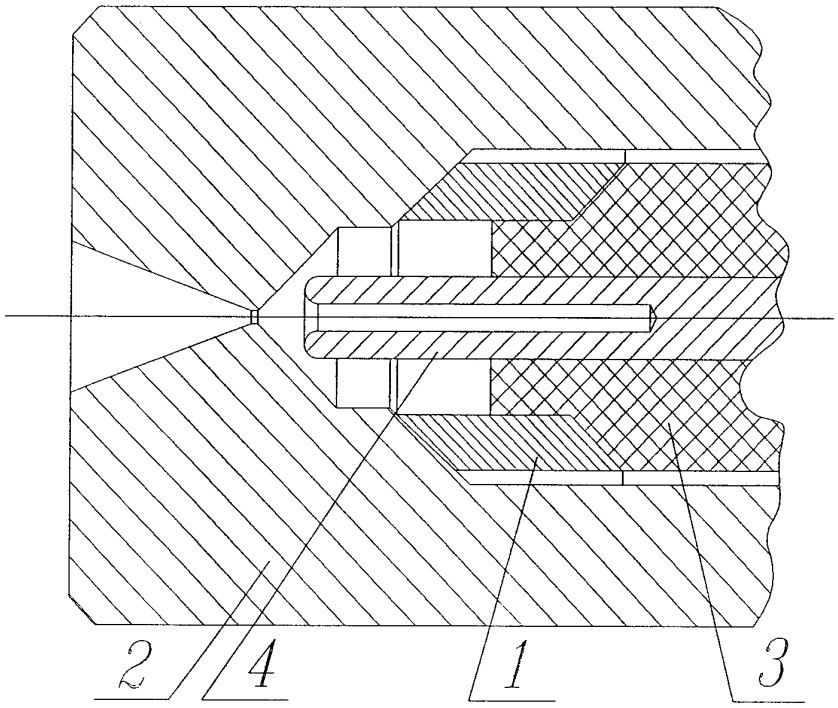

a - discharge chamber configuration
1 - injector, 2 - anode, 3 - insolator, 4 - hollow cathode;

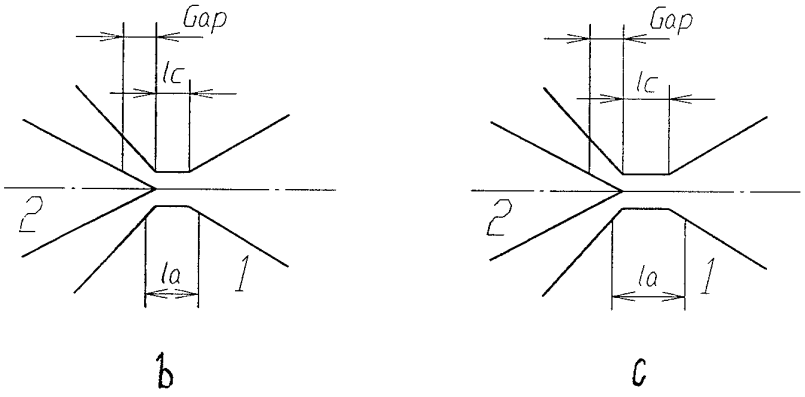

b, c - versions of the stick cathode installation.
1 - anode, 2 - cathode.

Fig. 20.

1 kW HOLLOW CATHODE ARCJET CONFIGURATION

(2-nd modification)

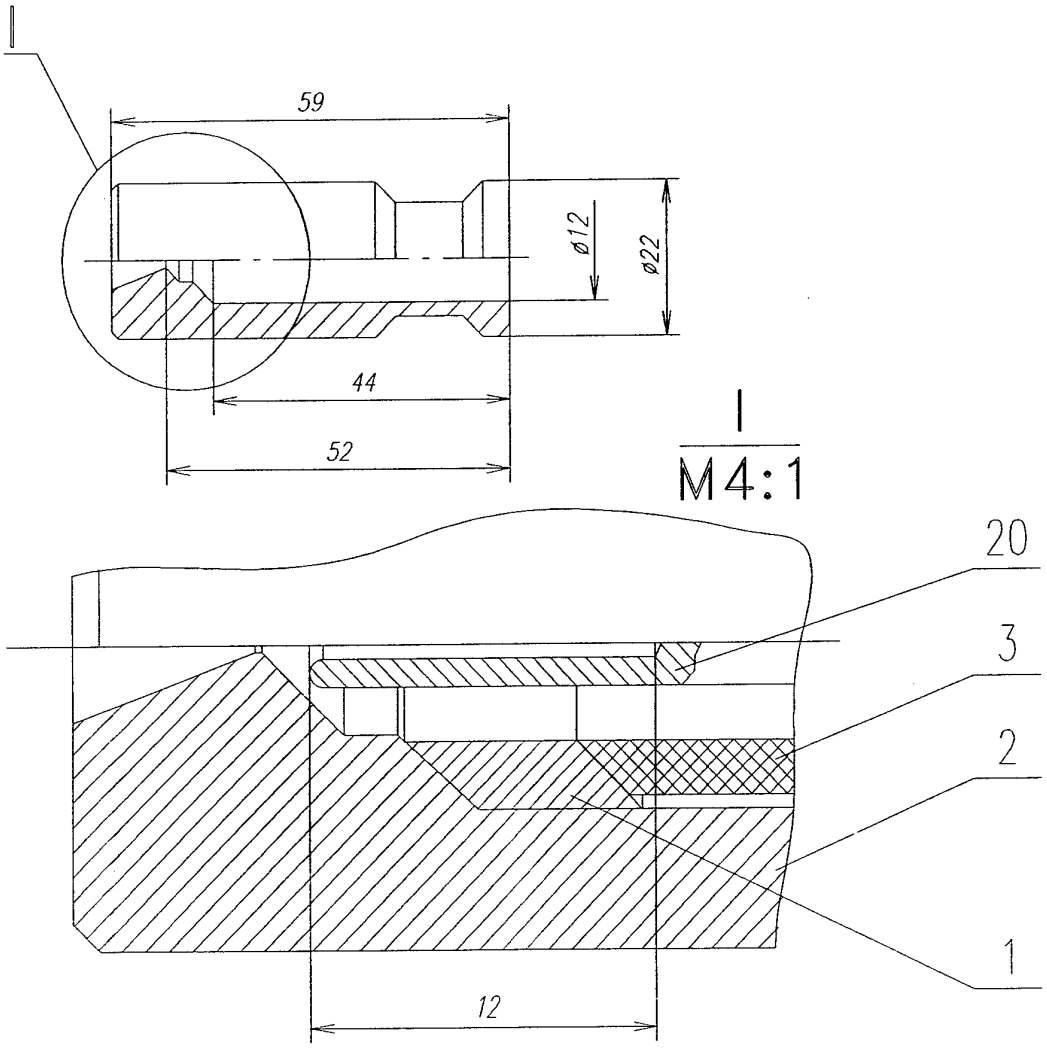

1 - injector, 2 - anode, 3 - insolator, 20 - hollow cathode

Fig. 21.

1 kW ARCJET EXPERIMENTAL SCHEME

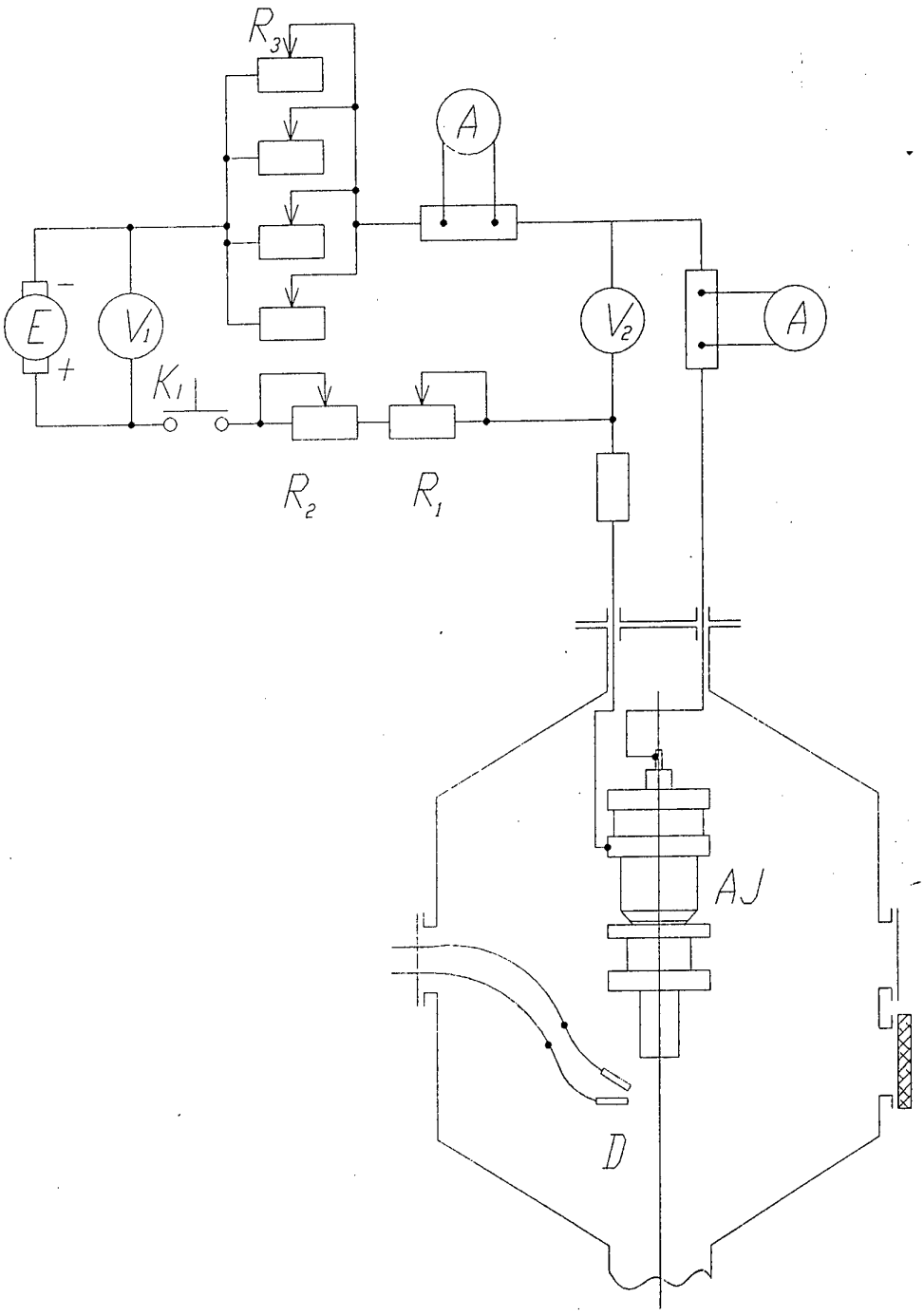

R_1, R_2, R_3, - resistors, AJ - 1 kW Arcjet, D - plasma ignitor

Fig. 22.

2.2.3. 1 kW arcjet integral parameters.

The investigation of the hollow cathode in the discharge at the pressure range 100...200 kPa was made for the first time. The main goal of the research was to show the hollow cathode efficiency under the given conditions and to determine the integral thruster performances, to reveal the conditions of stable homogenious discharge, to get the preliminary estimations of errosion rate of the cathode. The comparison of the W+2%La_2O_3 and W+3%ThO_2 cathodes were also revealed. Depending upon the test objectives the cathode operational time was from 4 to 50 hours.

Experimental dependences of voltage Ud (Fig. 23) and power N (Fig. 24) on discharge current Id for the cathodes of different materials at operating in N_2 are shown in Fig. 23,24.

Steady thruster operation was observed in current range of 7...25 A, power 0.5...1.4 kW under the pressures of 202...224 kPa and nitrogen flow rate 110 mg/s.

In hollow cathode arcjet similar to low power thrusters with rod cathode in approximately the same parameter range [10,11] the falling volt-amper characteristic is observed. The thoriated tungsten hollow cathode with the same cavity diameter (1.3 mm) demonstrated higher dischcarge voltages at the same current values (Fig. 23) than the W+2%La_2O_3 cathode. The current value of the discharge going out in the case of the thoriated cathode (10 A) is also higher than in the case of lanthanated cathode (7,5 A).

The influence of the cavity diameter in the limits 1...1.3 mm practically do not influenced on the VAC character.

50-hour tests at the given nitrogen flow rate 110 mg/s and discharge chamber pressure 203...224 kPa were made with the A-cathode. Test procedure included start up mode transition to the preliminary discharge mode by changing flow rate and heating for 30...40 min before the stationary heat regime. Then the nominal operational mode was being achieved with the following parametres:

- pressure 205 ± 5 kPa;
- consumption 110 ± 10 mg/s;
- discharge current 15 ± 0.5 A.

Under 50-hour tests of the W+2%La_2O_3 cathode the discharge current was kept up at 10 ± 0.5 A.

Discharge current changing was followed by both: discharge voltage and gas pressure changing. The average value of the magnitude $\Delta U/\Delta P$ at the current 15 A was approximately 0.4 V/kPa and of the magnitude $\Delta U/\Delta I$ was about 0.7 V/A. Thus set accurancy of the operational mode by voltage ± 2 V, and by current ± 0.35 A at the digital-device registration accurancy 0.01 V and 0,5 A.

After transition to the given operational mode its stability was provided by the gas feeding and vacuum pumping systems during the whole experimental time. Usually each test took 4...7 hours. 50-hour test were made without model resetting. In cases when the errosion

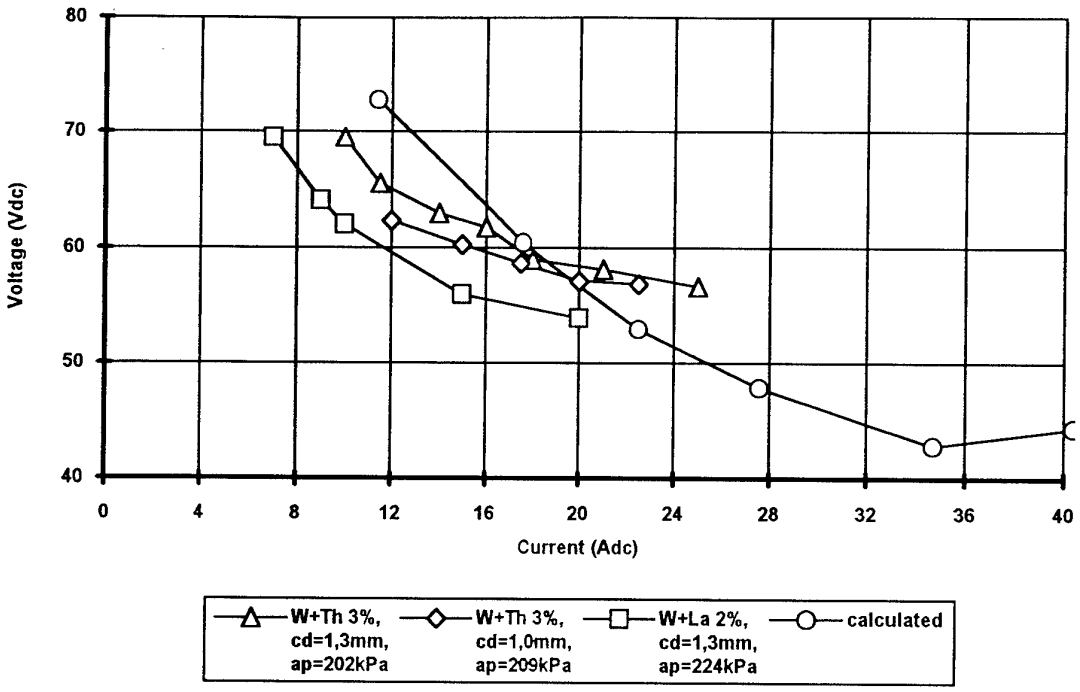

Nitrogen, flow rate 110 mg/s, constrictor diameter 0,8...1 mm, gap 0,2 mm.
(definitions: *cd* - cavity diameter; *ap* - average pressure)

Fig. 23.

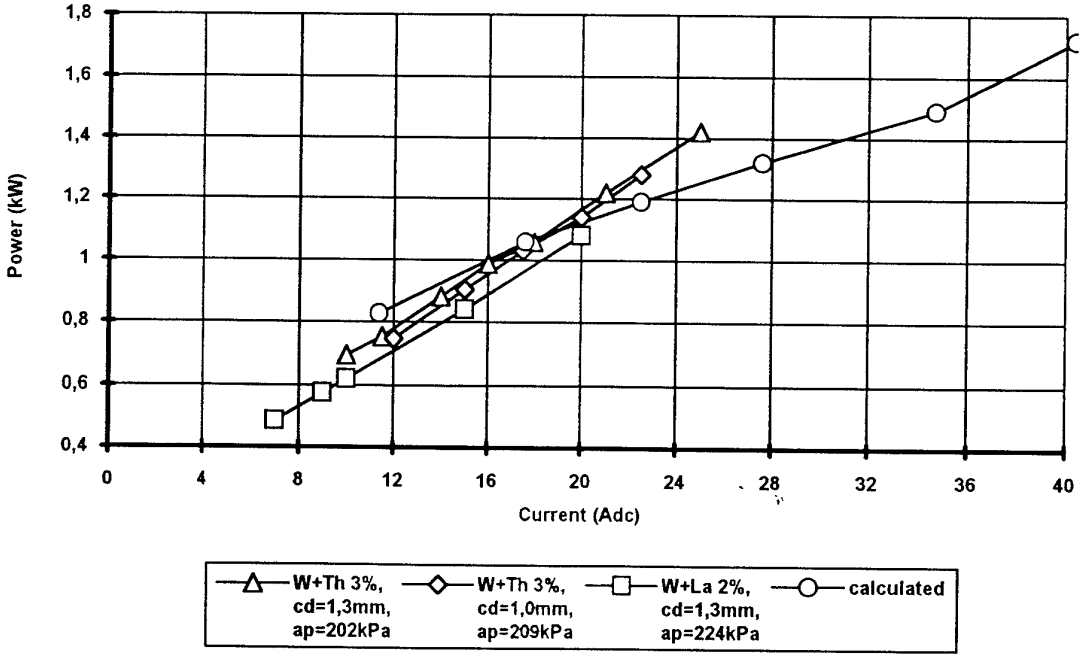

Nitrogen, mass flow rate 110 mg/s, constrictor diameter 0,8...1 mm, gap 0,2 mm.
(definitions: *cd* - cavity diameter; *ap* - average pressure)

Fig. 24.

analysis was necessary the resettings were unevitable. Nominal mode setting procedure was repeated after each resetting for example after the next working gas baloon replacement and after turning off the discharge.

Figures 25...32 show the typical discharge voltage and current time histories at the steady mode for different cathode work duration. In the refferences to the figures the average values and their mean-square deviations are given. We see a great discharge stability at the nominal modes. We should increase the pressure setting accuracy for a discharge pressure in the order of its value to keep the nominal mode parameters in the given limits 0.1...0.25 V.

2.3. Features of 1 kW arcjet hollow cathode erosion.

2.3.1. General erosion characteristics.

The hollow cathode erosion investigations in arcjet discharge under the pressure 100...200 kPa were made for the first time. Nitrogen under the pressure of 200 kPa and at the current value 10 A and 15 A was used in these tests.

Cathode erosion of the ($W+2\%La_2O_3$) cathode was studied for 50-hours at the discharge current value 10 A and discharge voltage 57 V (power is nearly 600 W). The thruster was not resetted during the whole 50 hours. Total number of starting up was 26. Average specific erosion was 5.8 10^{-11} kg/C. The longtitudinal section of the cathode after the test is shown on the photo in Fig. 34.

The initial form of the working tip was of truncated-cone-shape. Taking into account the test results the working tip form was similar to the one shown in the photo in Fig. 33a. The erosion of two other cathodes estimated at duration time tests of about 4 hours. The photos of the cathodes before and after the tests are shown in Fig. 33,34. We should notice that the cathode tip form was near to regular during the whole period of the tests. In the $W+2\%La_2O_3$ cathode test at the current value 15 A and power 825 W the forming of a "plug" at the cavity origin was observed as it is seen in Fig. 34.

The plug growing was noticed after the first 4 hours of the test. Such formation was not observed at the thoriated cathode even with more powerfull discharge: current 15 A, power 960 W. The average specific erosion of both cathodes was rather similar:

for ($W+2\%La_2O_3$) cathode - 1.7×10^{-11} kg/C,

for ($W+3\%ThO_2$) cathode - 2.0×10^{-11} kg/C.

2.3.2. Research on hollow cathode working surfaces.

Research on different parts of the cathode active zone was made using light and scanning electron microscopy.The cathode surface photos made by the light electron microscopy method are shown in Fig. 35,40.

The laminated material structure of the cathodes is clearly seen in the photos, it is typical for the technology of the thin sticks (3 mm) manufacturing. Probably this kind of

VOLTAGE TIME HISTORY AFTER 2,5 HOURS CATHODE B OPERATING TIME

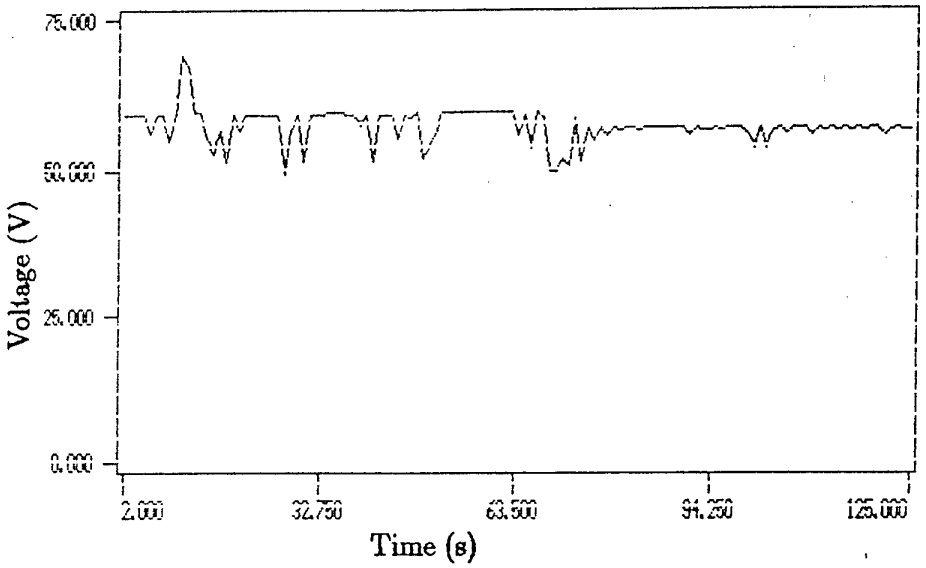

mean value U_d=57.5 V; mean-square error σ =0.251 V

Fig. 25.

VOLTAGE TIME HISTORY AFTER 5 HOURS CATHODE B OPERATING TIME

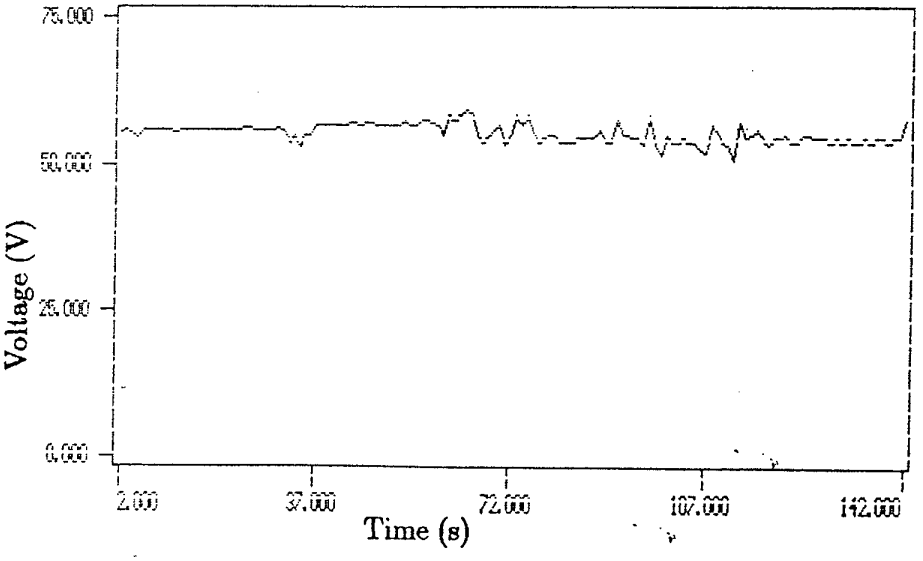

mean value U_d=55.5 V; mean-square error σ =0.128 V

Fig. 26.

VOLTAGE TIME HISTORY AFTER 7 HOURS 40 MINUTES CATHODE B OPERATING TIME

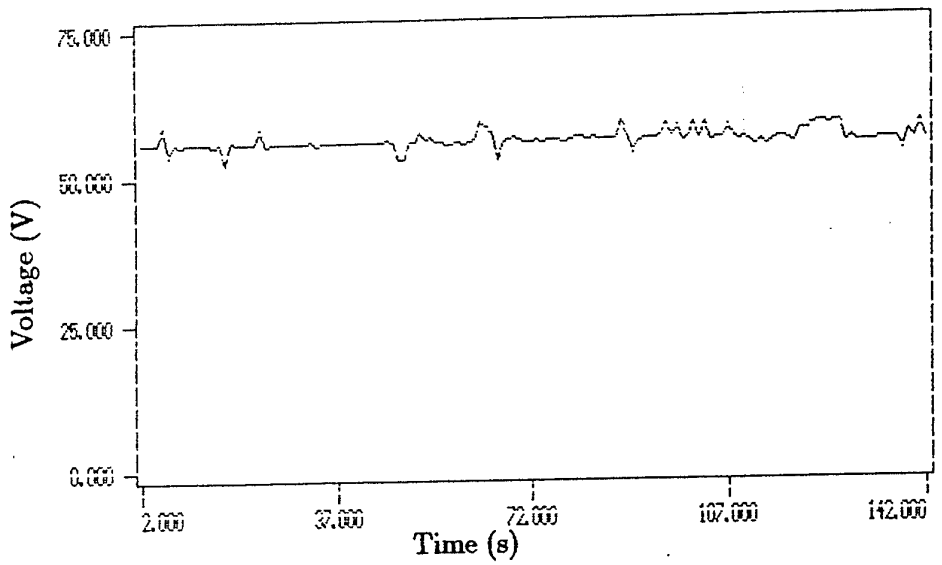

mean value U_d=56.4 V; mean-square error σ=0.101 V

Fig. 27.

CURRENT TIME HISTORY AFTER 8 HOURS CATHODE B OPERATING TIME

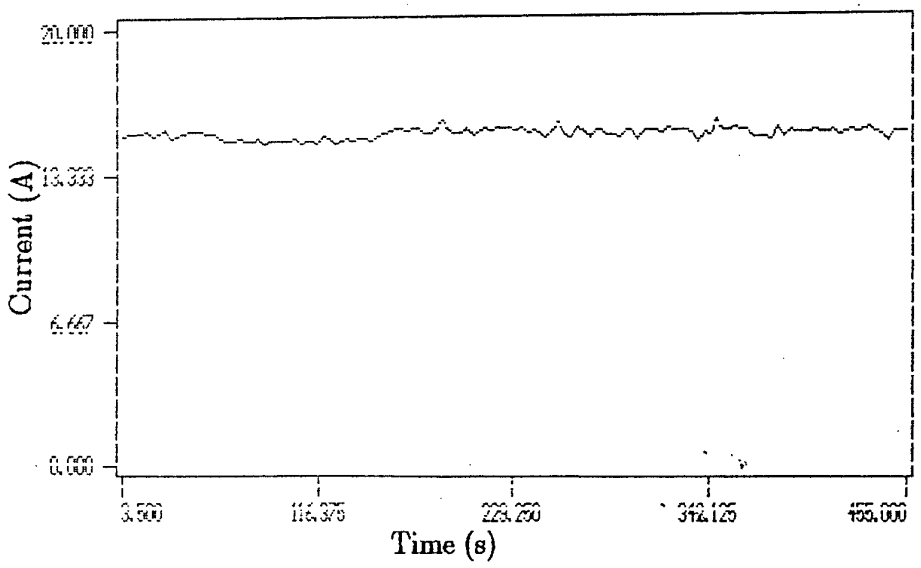

mean value I_d=15.2 A; mean-square error σ=0.021 A

Fig. 28.

VOLTAGE TIME HISTORY AFTER 14 HOURS CATHODE B OPERATING TIME

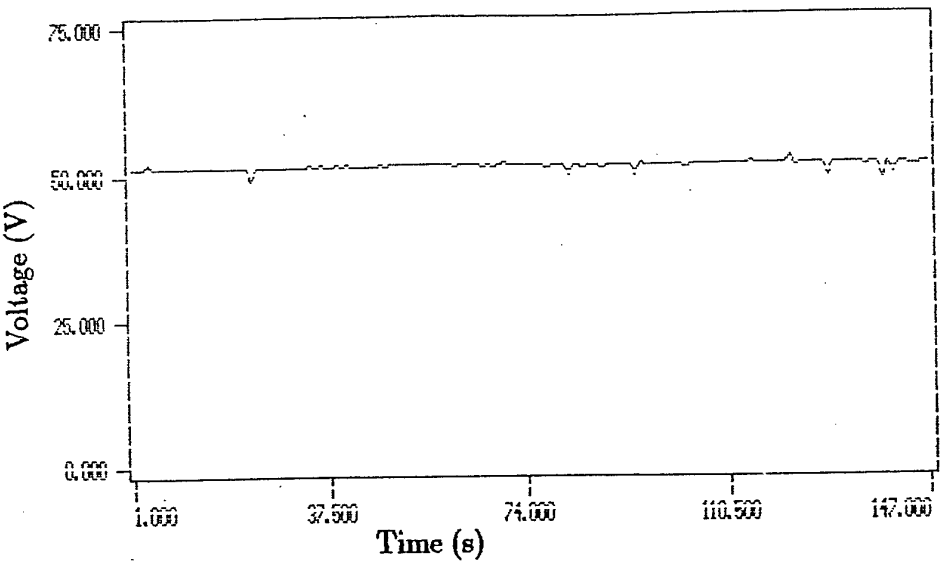

mean value U_d=51.42 V; mean-square error σ =0.033 V

Fig. 29.

CURRENT TIME HISTORY AFTER 14 HOURS CATHODE B OPERATING TIME

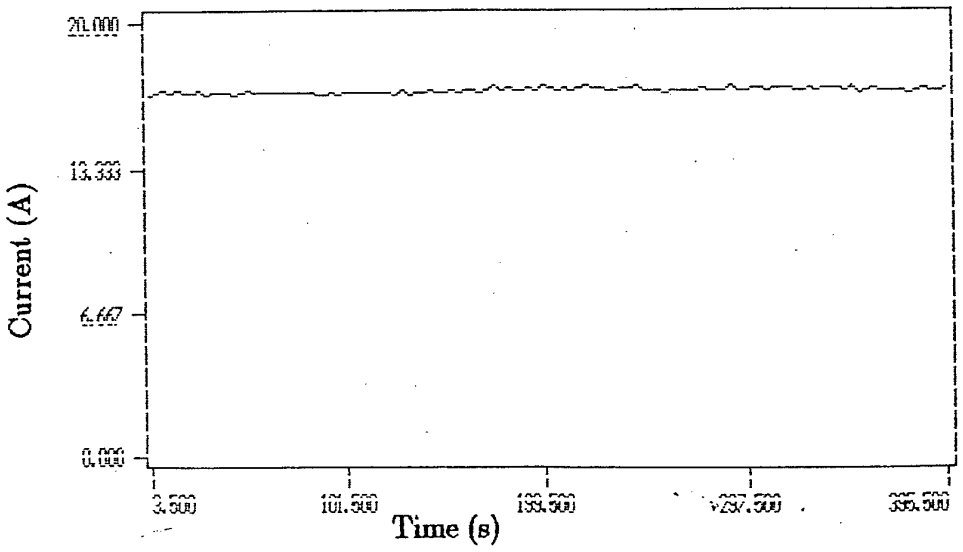

mean value I_d=16.84 A; mean-square error σ =0.012 A

Fig. 30.

VOLTAGE TIME HISTORY AFTER 3HOURS CATHODE C OPERATING TIME

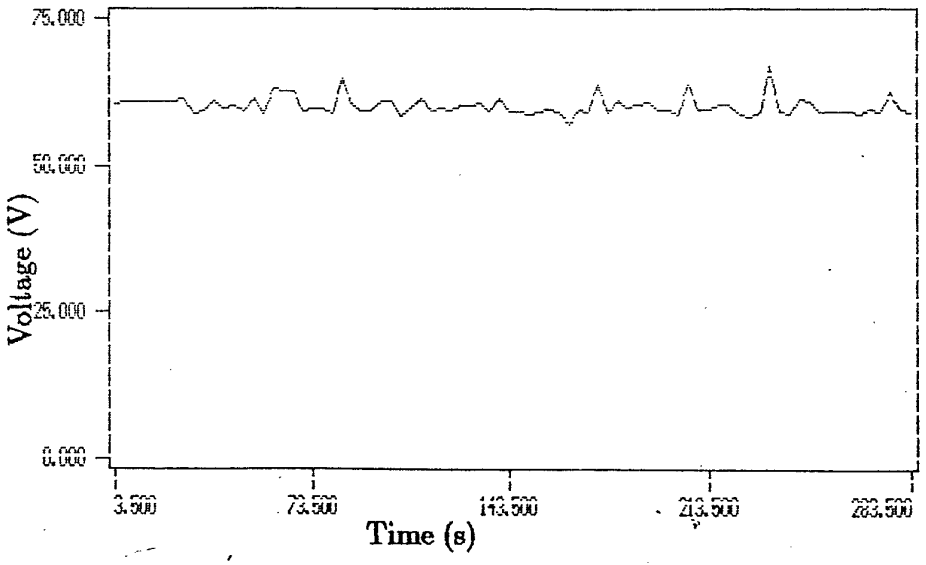

mean value U_d=60.4 V; mean-square error σ =0.174 V

Fig. 31.

VOLTAGE TIME HISTORY AFTER 3 HOURS CATHODE D OPERATING TIME

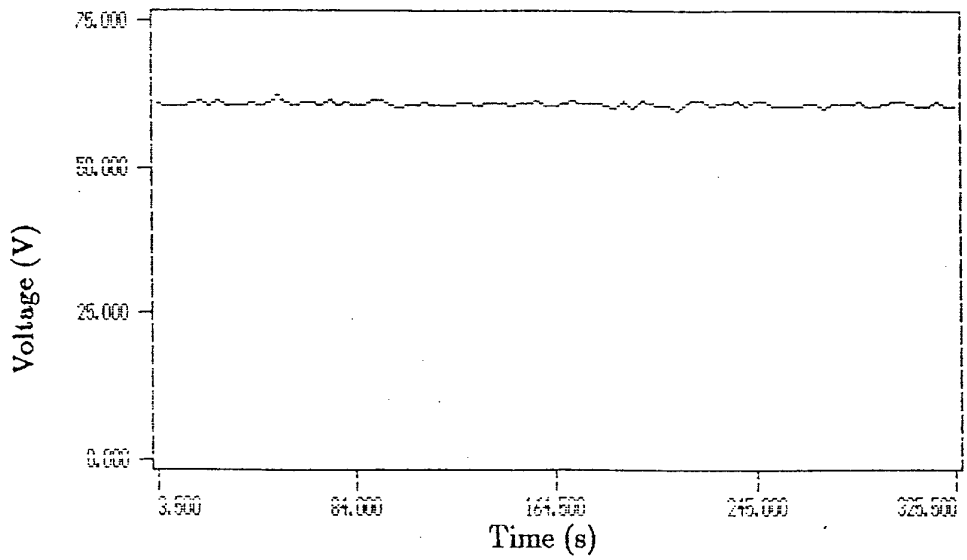

mean value U_d=61.16 V; mean-square error σ =0.045 V

Fig. 32.

TYPICAL EROSION 0F LOWER-POWER HOLLOW CATHODE (OUTWARD VIEW)

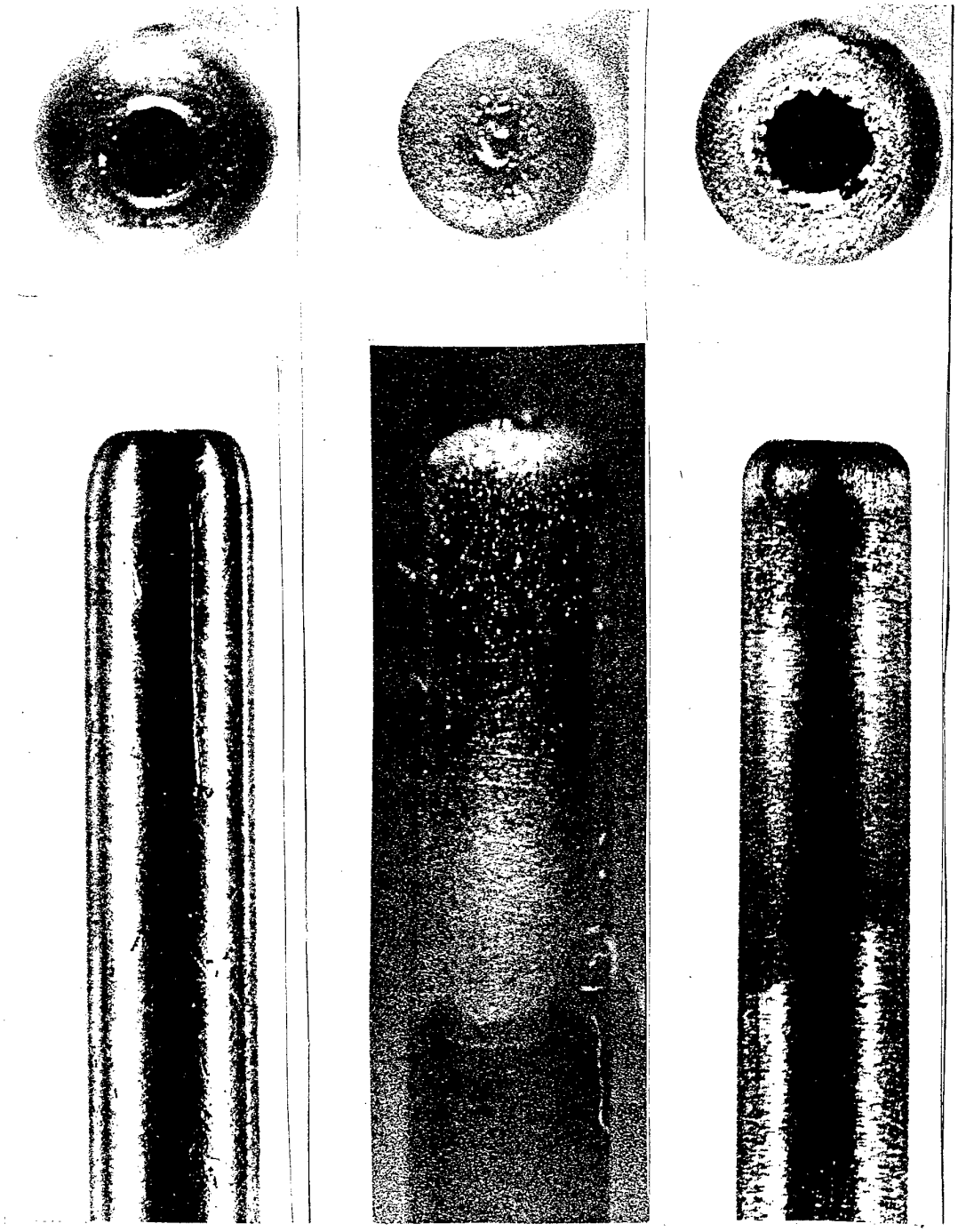

a) before tests

b) W + 2% La_2O_3
10 starts
30 hs
I_d=15 A
e.r. 1.7×10^{-11} kg/C

c) W + 3% ThO_2
8 starts
4 hs
I_d=16 A
e.r. 2×10^{-11} kg/C

N_2, P=200 kPa

Fig. 33.

TYPICAL EROSION 0F LOWER-POWER HOLLOW CATHODE (OF CAVITY)

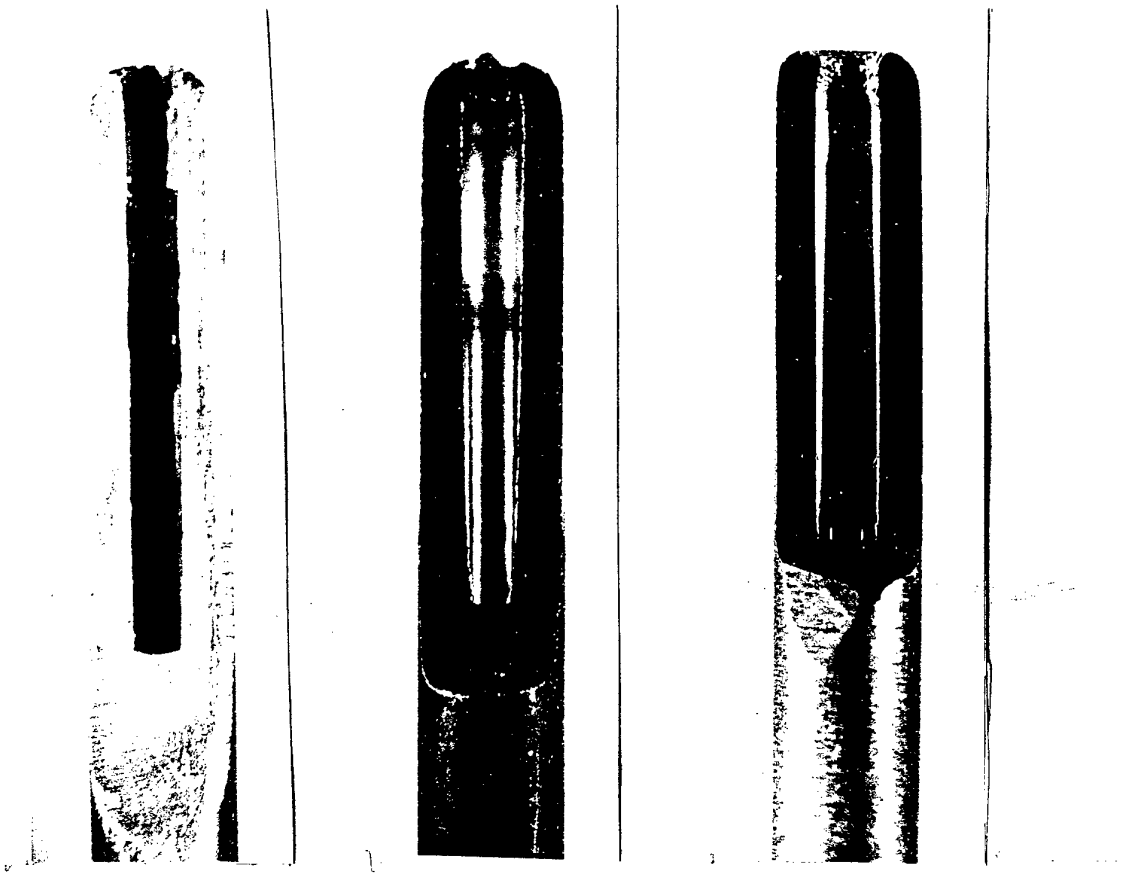

a) W + 2% La_2O_3
26 starts
50 h 15'
I_d=10 A
e.r. 5.8×10^{-11} kg/C

b) 30 - hours tests
W + 2% La_2O_3

c) 4 - hours tests
W + 3% ThO_2

Outward diam. 3 mm, Inner diam. 1.3 mm, N_2, P=200 kPa, U_d=60 V, I_d=15...16 A

Fig. 34.

structure influence on the properties of the cathode such as diffusion rate of light ionized additions (La,Th) to the cathode working surface and emission characteristics. Thus, as it is seen in Fig. 40,41, this structure cathode leads to the ($W+3\%ThO_2$) cathode tip deformation. The microphotos of the ($W+2\%La_2O_3$) cathode surface after 30-hour test in nitrogen are shown in Fig. 36,39. The uniform distribution of the erosion tracks along side and on inner surfaces are evident. Spectral analysis shows the presence of lanthan inclusions on the side surface (see Fig. 37). We can make an assumption that the erosion predominates over the condensation on the tip and side cathode surfaces, though near the plug the condensation can dominate. The photo of the inner surface and the plug (Fig. 37,39) indicates the complicated physical and chemical processes in the cavity. All the photos show a good discharge uniformity of the cavity surface erosion. A boundary of the active surface zone inside the cavity is observed distinctly in Fig. 41. It is located approximately a cavity diameter from the cathode tip. The comparision of Fig. 42,43 and 37,38 for thoriated and lanthanated cathodes shows that the thoriated cathode structure is grained finer. Thorium inclusions were revealed on the cavity surfaces (Fig. 44).

One of the most important goals of the further research is a more detailed analysis of the surface processes at high nitrogen pressures in hollow cathodes in the comparison with the processes in hydrogen containing gases.

3. COMPARATIVE ANALYSIS ON ARC JET THRUSTER PERFORMANCES WITH HOLLOW AND ROD CATHODES.

The arcjet discharge parametres may be estimated by the simple single-dimension semiempirical model, based on the well-known experimental data (see, for intance, [34,35]).

In single-dimension approximation we operate with environment parameters moreover their values are taken as averaged on cross and longitudinal section of a cylindrical arcjet channel. The calculation of the radial parameter distribution may be done in the first approximation by taking into account the effective cross-section area of the electroconducting arc channel through which the current flows and where Joule heating of the working gas takes place. This magnitude is expressed by constrictor cross-section area s_c, using the ratio $s_\sigma = \alpha_1 s_c$, where α_1 - is a nondimensional empirical factor < 1 (~0.16...0.25) [35]. The analysis shows that the transition of subsonic stream to supersonic one takes place behinde the constrictor channel {5,7,8]. This fact was taken into account due to another empirical factor $\alpha_2 = s_p / s_c$, where s_p - flow cross section in the transition area.

In one dimensional approximation we use the effective channel length La. This magnitude is a sum of the constrictor length, the distance between the cathode tip and the constrictor inlet cross-section and the distance between the constrictor outlet and the transition area cross-section.

Energy losses are taken into account by putting an energy efficiency η_e into the code. While voltage estimation we should calculate the sum of anode and cathode voltage bias.

LIGHT MICROSCOPY OF W + 2% La_2O_3 HOLLOW CATHODE

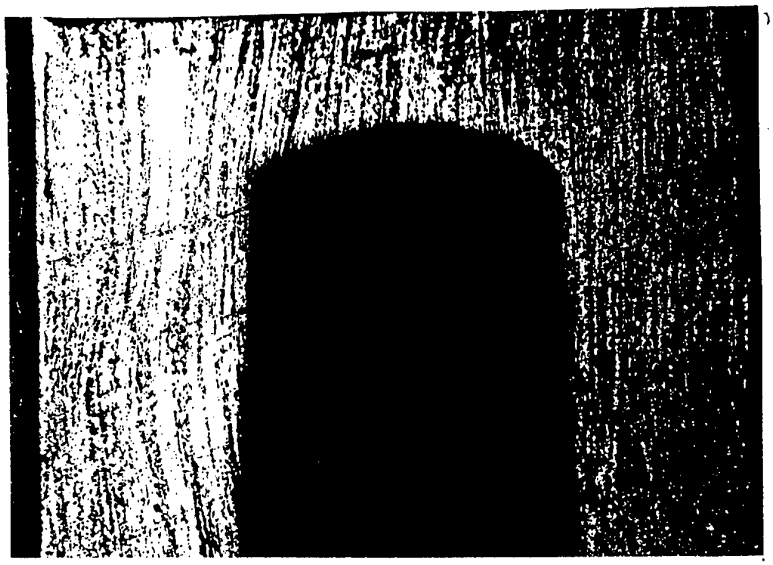

upper part x 50

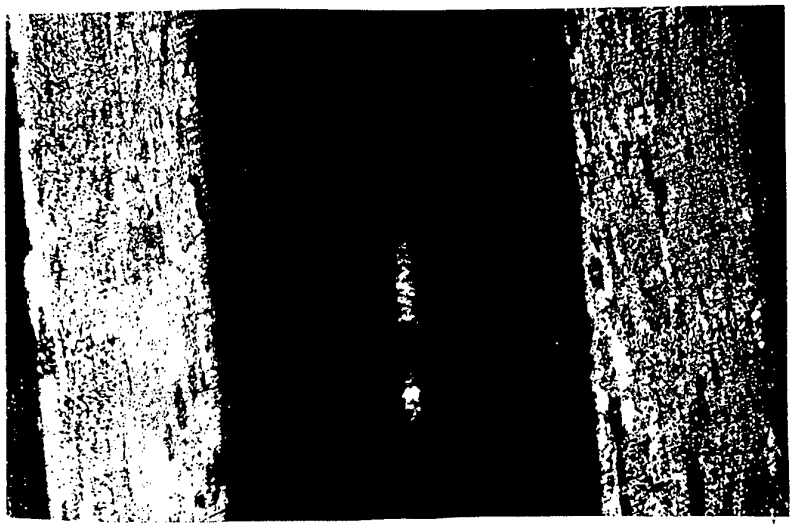

middle part x 50

working tip x 50

Fig. 35.

SCANNING ELECTRON MICROSCOPY OF W + 2%La_2O_3 HOLLOW CATHODE

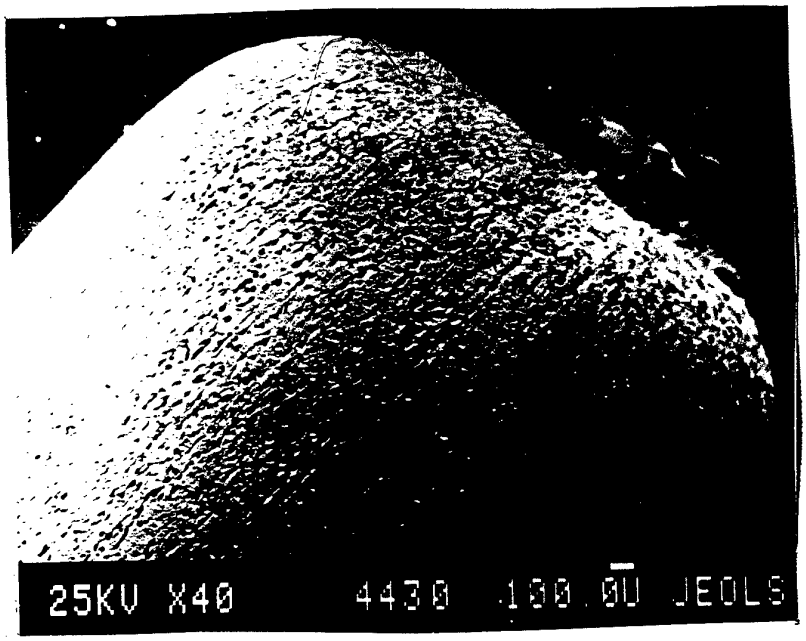

a - side view

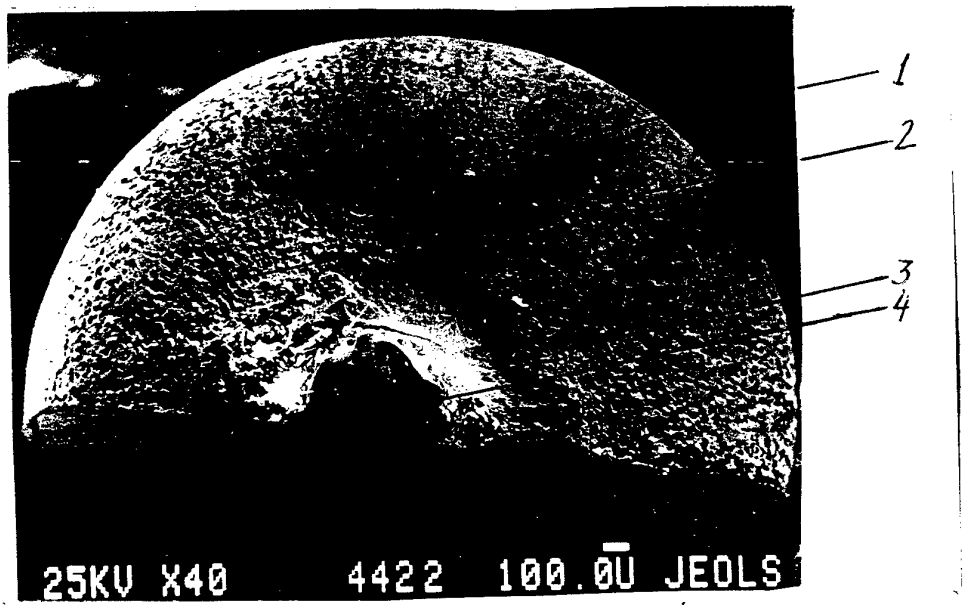

b - top side, 1,2,3,4 - scanning regions

Fig. 36.

SCANNING ELECTRON MICROSCOPY OF EXTERNAL SURFACE

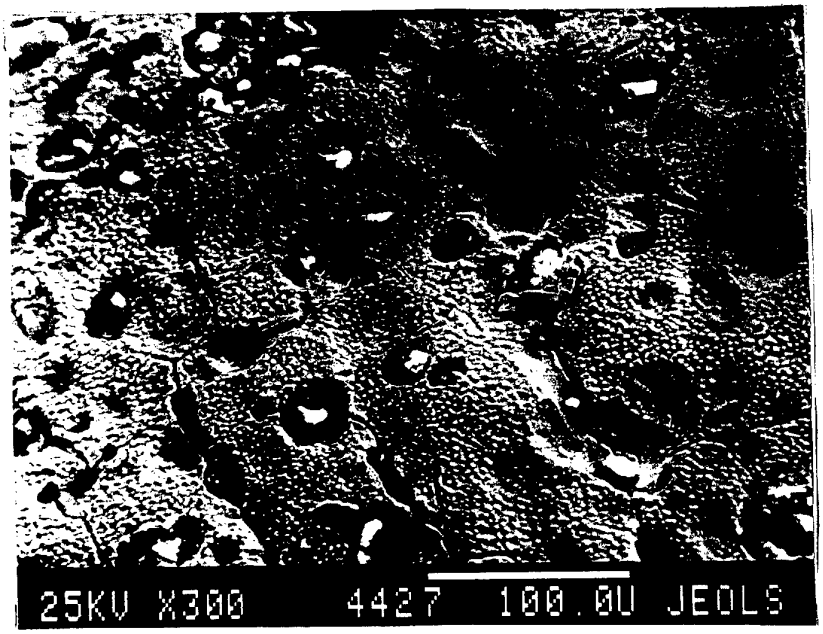

a - region 1 (Fig. 36)

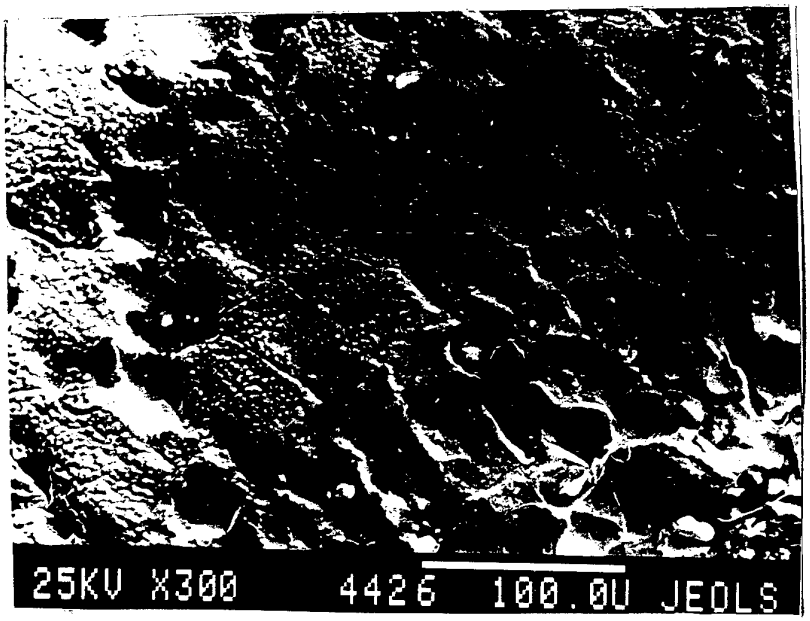

b - region 2 (Fig. 36)

Fig. 37.

SCANNING ELECTRON MICROSCOPY OF EXTERNAL SURFACE

a - region 3 (Fig. 36)

b - region 4 (Fig. 36)

Fig. 38.

SCANNING ELECTRON MICROSCOPY OF INNER SURFACE W + 2%La_2O_3 HOLLOW CATHODE

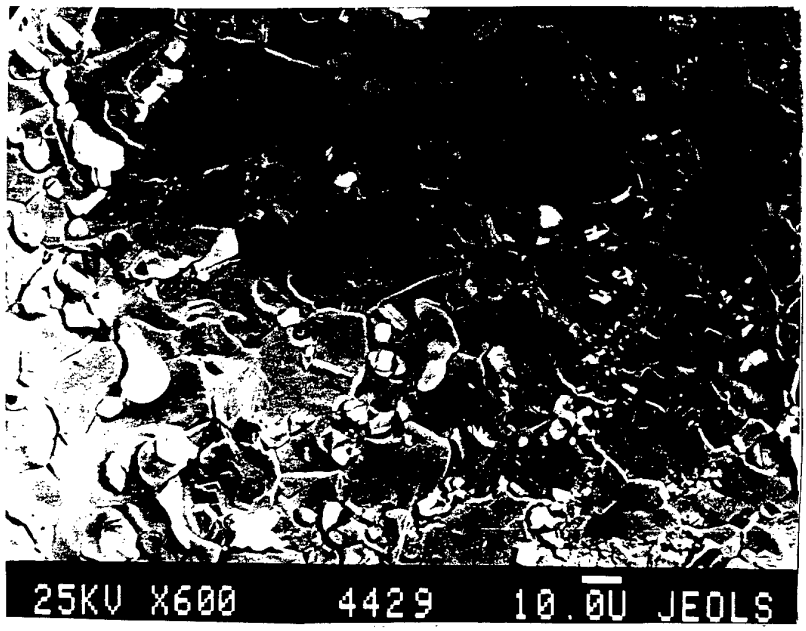

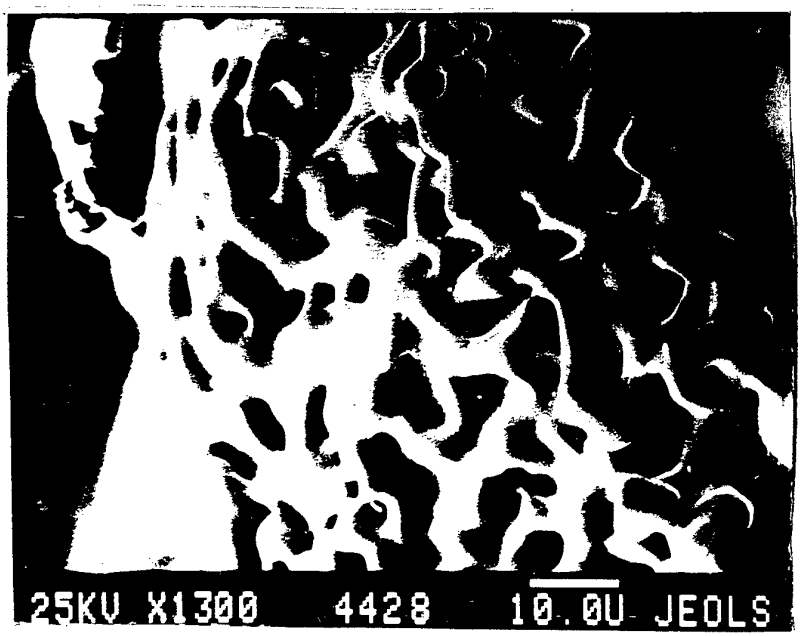

Fig. 39.

LIGHT MICROSCOPY OF W + 3%ThO_2 HOLLOW CATHODE CAVITY

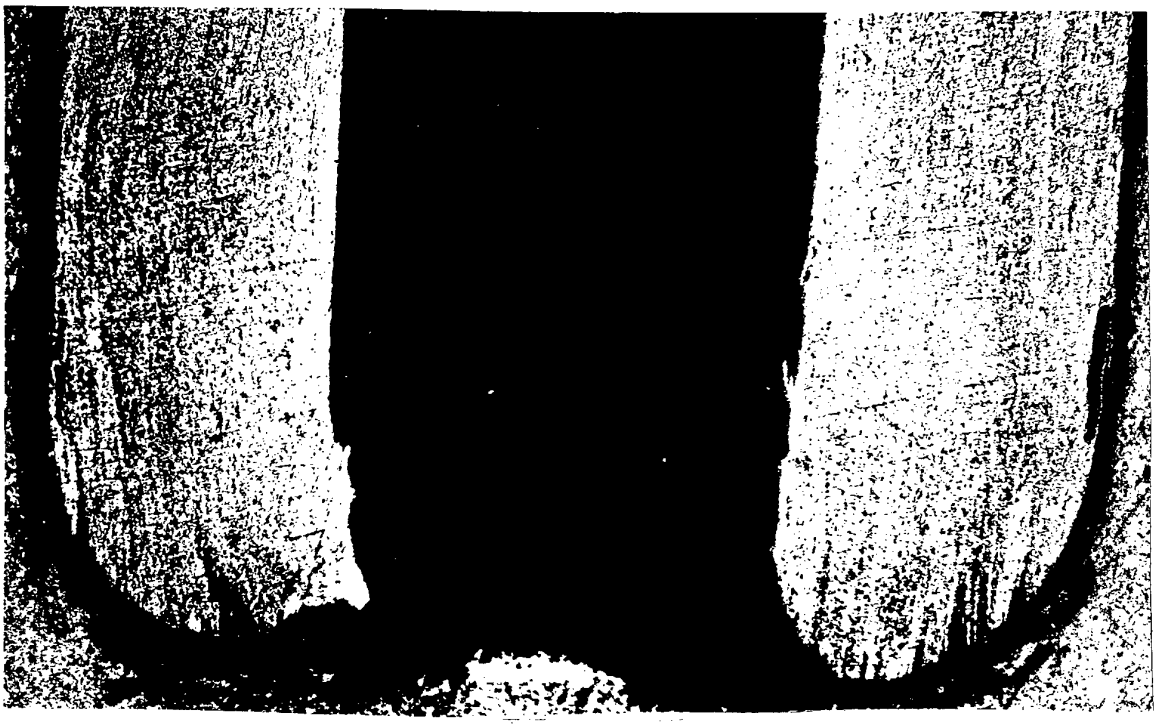

x 200

x 500
Working tip.

Fig. 40.

SCANNING ELECTRON MICROSCOPY OF W + 3%ThO_2 HOLLOW CATHODE

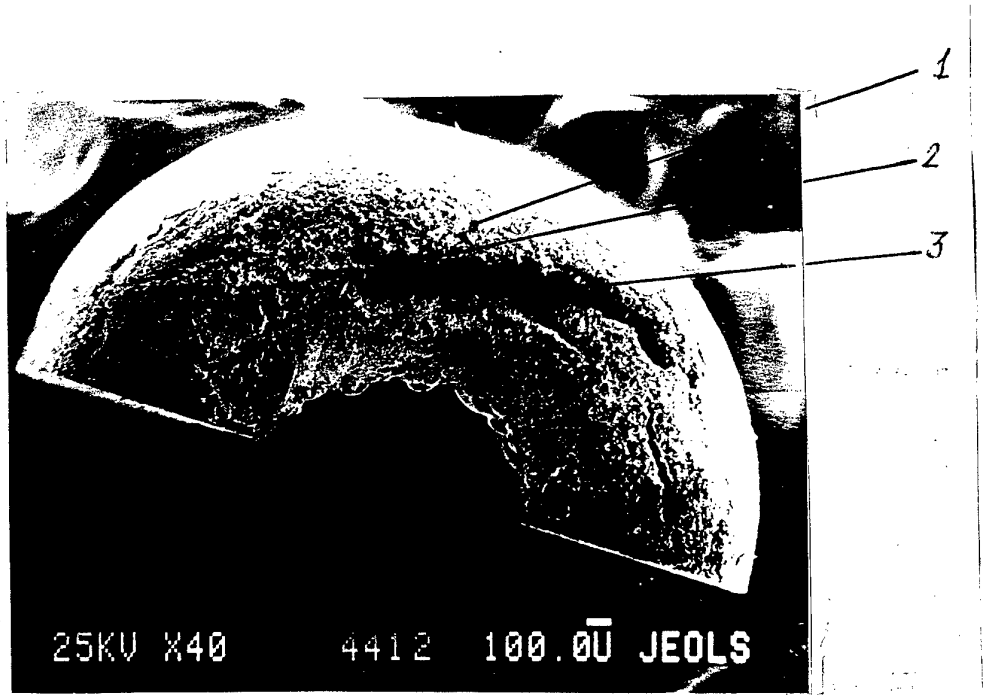

a - external surface, 1,2,3 - scanning regions

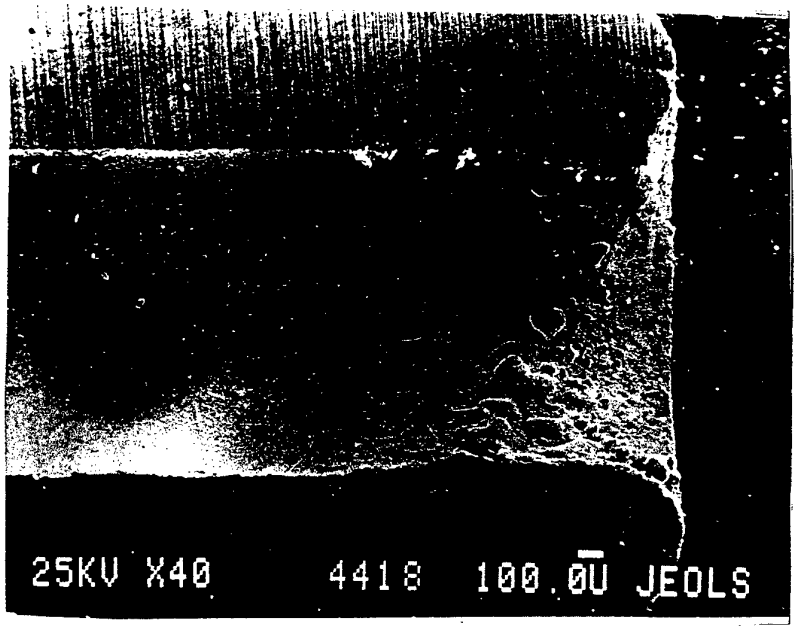

b - inner surface

Fig. 41.

SCANNING ELECTRON MICROSCOPY OF W + 3%ThO_2 CATHODE

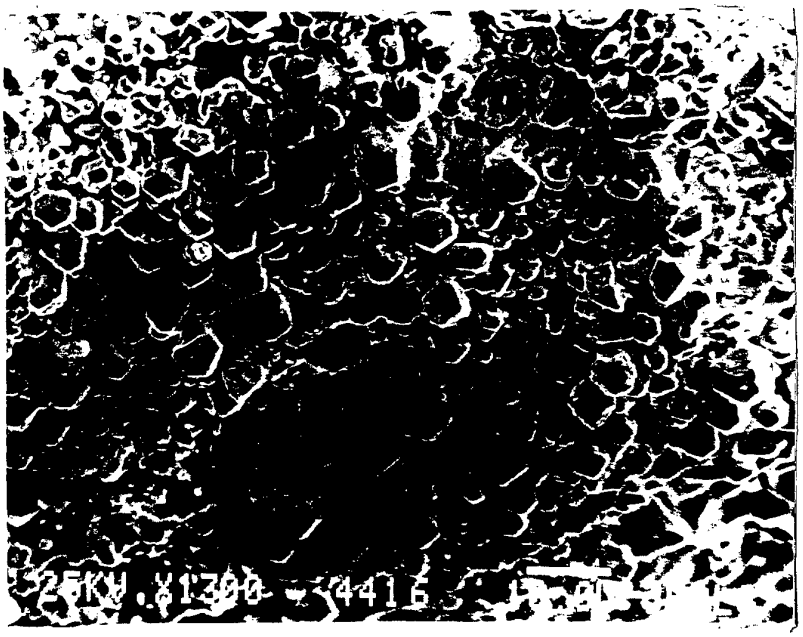

a - region 1 (Fig. 41)

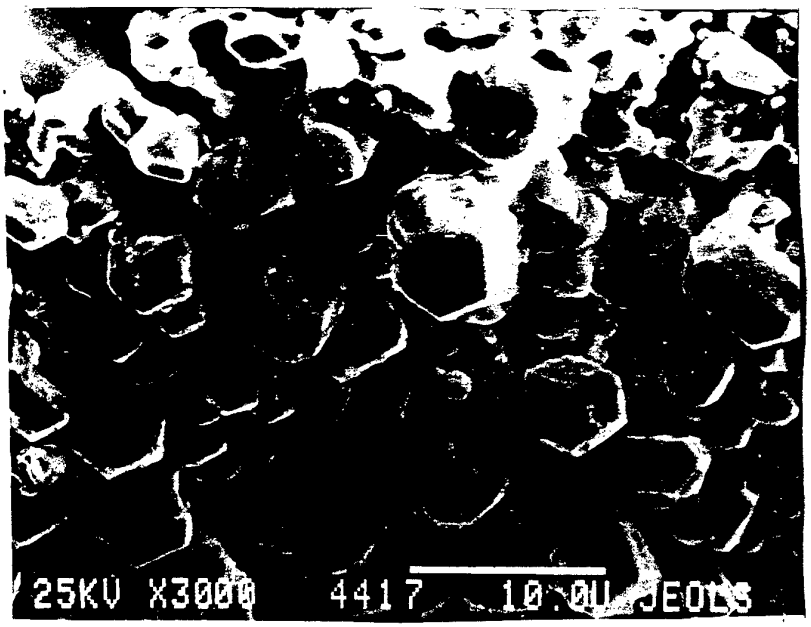

b - region 2 (Fig. 41)

Fig. 42.

SCANNING ELECTRON MICROSCOPY OF W + 3%ThO_2 HOLLOW CATHODE CATHODE EXTERNAL SURFACE

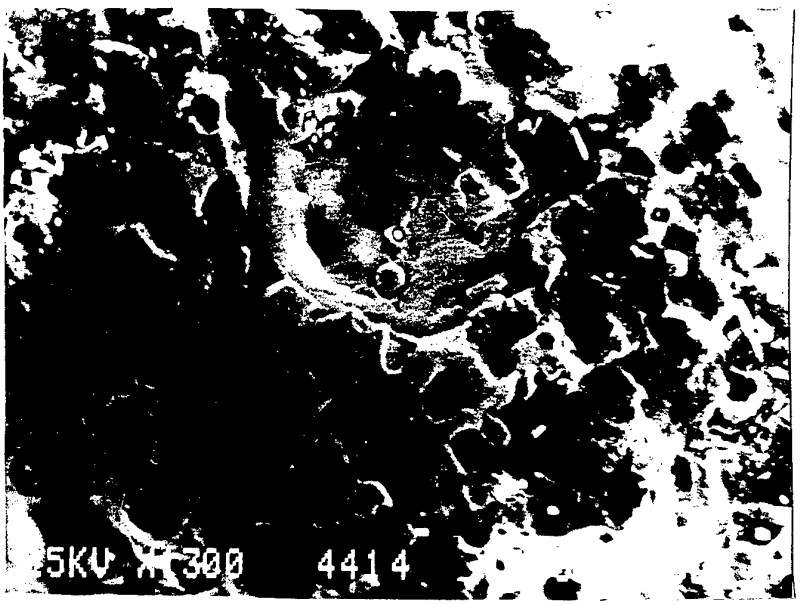

a - region 2 (Fig. 41)

b - region 3 (Fig. 41)

Fig. 43.

SCANNING ELECTRON MICROSCOPY OF W + 3%ThO_2 HOLLOW CATHODE

a - external surface

b - inner surface

Fig. 44.

According to the well-known experimental data [34,35] this magnitude is about 12...15 V for average pressure and different cathode materials.

On the base of the equations of the energy and impulse balances we can write the continuum equation in one-dimension approximation in the following form:

- pressure $P = \frac{G}{\alpha_2 s_c}\left(\frac{RT}{\gamma M}\right)^{\frac{1}{2}}$ (1)

- enthalpy $H = H_T + \frac{U_s^2}{2}$ (2)

- discharge power $N = \frac{\alpha_1}{\eta_e} GH$ (3)

- voltage $U = \left(\frac{GHl_a}{\eta_e s_c \sigma} + \left(\frac{\Delta\varphi}{2}\right)^2\right)^{\frac{1}{2}} + \frac{\Delta\varphi}{2}$ (4)

- current $I = N / U$ (5)

These ratios allow to estimate Volt-Ampere (VAC) and Watt-Ampere (WAC) characteristics at the fixed gas temperature T and mass flow rate G also using the codes for calculation of such thermodynamic parameters as:

- molar mass - M
- adiabatic exponent - γ
- sonic velocity u_s
- enthalpy H_t
- specific electroconductivity - σ

The last value for number of a gases and their mixtures was kindly given by the colleagues from CENTROSPAZIO.

For the regims at the pressure nearly of 100 kPa the thermodynamic parameters were determined supposing thermodynamic equilibrium. For arcs at average pressure the empircal parameters were taken: α_F=0,16 [12], α_2=1.2 and $\Delta\varphi$ = 15 V [34,35].

The calculated V-I and N-I characteristics for nitrogen at η_e = 0,8 are presented in Fig. 23, 24. Parameter la was equal 0.6 mm, r_c=0.5 mm. The average calculated pressure was 213 kPa. The experimental V-I and N-I caracteristics for low power rod cathode AJT for (N_2+2H_2) are given in [10].

V-I and N-I calculated characteristics for two different electrode systems with la parameter varied closely to its experimental values are also given in Fig. 45, 46. Similarity of these experimental and calculated dependences was satisfactory. It allows us in the first approximation using experimental value of specific power N/G and calculated value of enthalpy H to determ the dimensioneless parameter α_1 / η_e from eq. 3.

The results of the calculation for hollow and rod cathode AJT in current range 10...25 A are given in Fig. 47. One can see that the specific power for (N2+2H2) mixtures is more than 2 times higher than for pure nitrogen. This fact is explained by the effect of higher level of enthalpy in the first case.

1 KW SIMULATED HYDRAZINE ARCJET V-I AND N-I CURVES AT MASS FLOW RATE 50 mg/s, CONSTRICTOR DIAMETER AND LENGTH 0,54 mm, GAP 0,45 mm

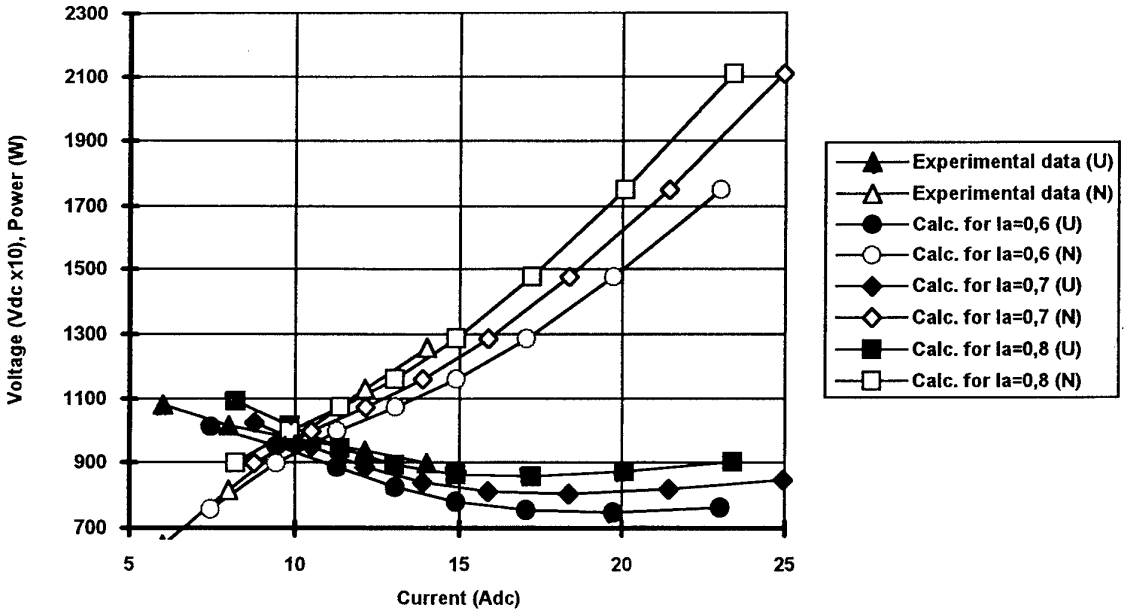

Fig. 45.

1 KW SIMULATED HYDRAZINE ARCJET V-I AND N-I CURVES AT MASS FLOW RATE 50 mg/s, CONSTRICTOR DIAMETER 0,51 mm AND LENGTH 1,0 mm, GAP 0,45 mm

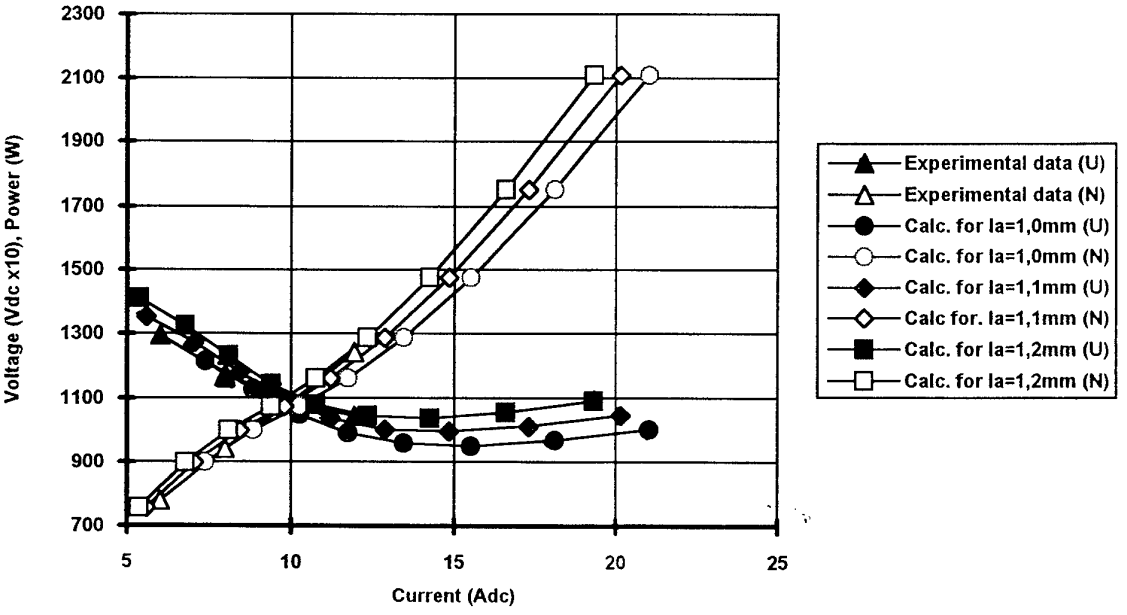

Fig. 46.

DEPENDANCE OF SPECIFIC POWER ON TOTAL ENTHALPY FOR 1 KW ARCJET

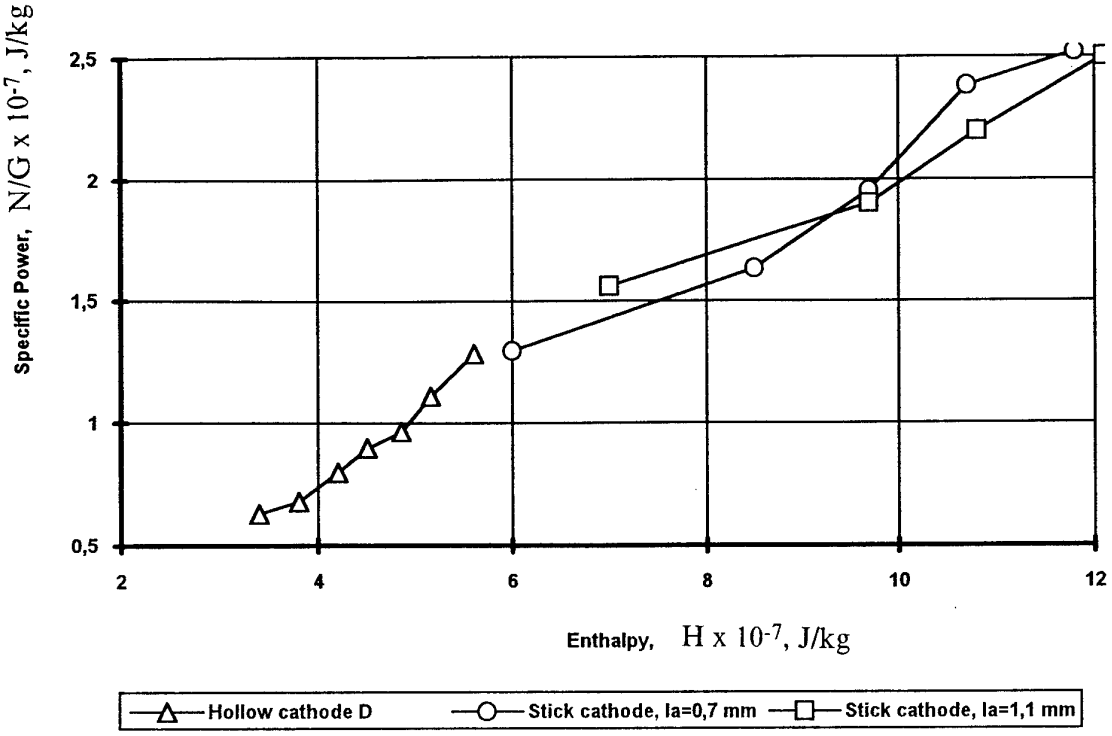

N_2, flow rate 110 mg/s

N_2+2H_2 mixture, flow rate 50 mg/s

N_2+2H_2 mixture, flow rate 50 mg/s

Fig. 47.

As it follows from figure 47 parameter α_1 / η_e in given current range is does not depend on discharge current for given electrode system design. Linear approximation of these dependences gives the following values of α_1 / η_e parameter: for hollow cathode AJT - 0.318, for rod cathode AJT - 0.208. This result shows the better filling of the arc channel by plasma in the case of a hollow cathode.

In the case of a rod cathode the value α_1 / η_e for different electrode system configurations is close to taken for calculated values of the α_1 and η_e parameters: $\alpha_1 = 0.16$ and $\eta_e = 0.8$.

Good agreement between experimental and calculated VIC and WIC allows us to be assured in the estimation of non-measured parameters such as: enthalpy, ionisation ratio, plasma components etc. One can estimate arc channal flow enthalpy and specific power for N_2 and (N_2+2H_2) mixtures from data of Fig. 47. For example ionization ratio for (N_2+2H_2) mixture is about 0.003at H~10^8 J/kg, N~10^3 W, N/J~2x10^7 J/kg. The average gas temperature in the arc channel is above 9000 K. Dissotiation ratio is nealy 1.

Thus the given semiempirical analysis allows us to judge by the main working processes in hollow cathode arcjets as well as general thruster characteristics and efficiency.

CONCLUSION

1. High current arc discharges in nitrogen, argon and (Ar+He) mixture in current range 200...1200 A and pressure range 10...50 kPa has been investigated. It is shown that hollow cathodes of designed type be assembled with arcjet thrusters of power lavel 10...50 kW.

2. Different hollow cathode units has been designed and tested. The hollow cathode discharge start up procedure has been developed.

3. Single-channel hollow cathodes formed by a system of sticks has been designed and tested for high-current arcjet middle power plasma generators and thrusters.

4. Cathode erosion peculiarities for middle power thrusters has been strudied. Total operational time of some cathodes is more than 250 hours and they keep their work capability. Specific ($W+2\%La_2O_3$) cathode erosion is $5x10^{-12}$ kg/s for (Ar+He) mixtyre.

5. For the first time low-power hollow cathode arcjet has been tested in nitrogen at pressure 100...200 kPa in current range 10...25 A (discharge power 0.5...1 kW).

6. Four hollow cathodes were designed for 1 kW power thruster and the hollow cathode effect was demonstrated under the given conditions.

7. ($W+2\%La_2O_3$) and ($W+3\%ThO_2$) hollow cathodes with 3 mm outer diameter and 1...1.3 mm cavity diameter has been tested in 1 kW thruster operating in nitrogen. All cathodes demonstrated thruster operation with uniform distributed discharge. Current and discharge voltage stability corresponds to root - mean - square deviation value 0.15...0.2%.

8. Endurance 50-hour tests were made for a $W+2\%La_2O_3$ cathode at 26 startings.

9. The special features of 1 kW arcjet hollow cathode erosion has been researched with the help of electron microscopy for 1 kW thruster. The average specific erosion was within $1.7x10^{-11}$ kg/C ... $20x10^{-11}$ kg/C at nominal operational modes.

10. The semiempirical simulation model has been developed for low (~1 kW) and average (10...50 kW) power thruster parameter estimation.

REFERENCES

1. Vaulin E.P., Odintsova J.A. Diagnostic of inert gas plasma flows by spectrographic methods. Low-temperature plasma generators. "Energy". Moscow, 1969. p 446.

2. Vaulin E.P., Odintsova J.A. Some questions of gas mixture plasma flowing into vacuum. Low-temperature plasma generators. "Energy", Moscow, 1969, p 95.

3. Vaulin E.P., Obukhov V.A., Petukhov N.V., Feoktistov L.V. Arcjet plasma generator of average power with hollow cathode. 3-rd Germany-Russian conference on electric propalsion and their technical applications Stuttgart, Germany, 1994, paper.

4. Vaulin E.P., Kiruyshkina M.V., Latyshev L.A., Tikhonov V.B., Filatova E.A. Engineering methods of hollow cathode calculation. IEPC-93-019, 23-rd IEPC, September, 1993.

5. Polk J.E. and Goodfellow K.D. Results of a 1462 Hour Ammonia Arcjet Endurance Test. AIAA 92-3833, 28-th Joint Propulsion Conference and Exhibit. July, 1992.

6. Harris W.J., O'Hair E.A., Hatfield L.L., Kristiansen M. Cathode erosion research on medium to high power arcjet thrusters. IEPC-93-028, 23-rd IEPC, September, 1993.

7. Andrenucci M., Saccoccia G., Baiocchi G., Pezayna C., "Experimental Performance of a 1 kW Arcjet", AIAA 90-2583, 21-st IEPC, July, 1990.

8. Capecchi G., Scortecci F., Repola F. and Andrenucci M., "Parametric Test Results of a Low Power Arcjet", AIAA 93-213, 23-rd IEPC, September, 1993.

9. J.L. Delcroix, H.Minoo, A.R. Trindade. Etablissement d'une regle generale pour une decharge d'arc cathode creuse. J.Phys (Paris), 1968, v. 29, p 605-612.

10. J.L. Delcroix, A.R. Trindade. Hollow cathode arcs. Adv. in Elect. and Elect.Phys., 1974, v. 35, p 87-190.

11. A.Brunet. Hollow cathode arc. Effect of the cathode material on the internal plasma. Proc. XII Int. Conf. on Phenomena in Ionized Gases, Eindhoven, Holland, 1975, p 231.

12. A.Brunet. Hollow cathode arc. Experimental study of the plasma inside the hollow cathode. Rev. Phys. Appl., 1977, v. 12, p 1105-114.

13. C.M.Ferreira, J.L. Delcroix. Theory of the hollow cathode arc. J.Appl.Phys., 1978, v. 49, 2380-2395.

14. Buksht F.Y., Ribakov A.B. Hollow cathode theory with fully ionized dense plasma in arc mode. ЖТФ, 1978, v. 48, N 2, p 234-243.

15. Buksht F.Y., Ribakov A.B. Arc mode theory in hollow cathode. ЖТФ, 1978, v. 48, N 4, p 700-706.

16. Buksht F.Y., Ribakov A.B. The influence of surface emission properties on arc hollow cathode parametres in caesium plasma. ЖТФ, 1981, v. 51, N 9, p 1846-1849.

17. Dugev Y.A., Starcev E.A., Yeurgev V.Y. Physical processes in arc hollow cathode with highly-ionized dense plasma. ЖТФ, 1978, v. 48, N 10, p 2027-2039.

18. Dugev Y.A., Starcev E.A., Shkolnik S.M., Yeurgev V.Y. Low-temperature erosion free cathode at high current densities. ЖТФ, 1978, v. 48, N 10, p 213-216.

19. Dugev Y.A., Starcev E.A., Shkolnik S.M. Hollow cathode current limitation at low pressures. ЖТФ, 1978, v. 48, N 12, p 2495-2499.

20. Dugev Y.A., Mitrophanov N.K. Arc discharge with hollow cathode at average pressures. ЖТФ, 1978, v. 48, N 12, p 2500-2508.

21. Vaulin E.P. Some theoretical and methodical questions of design of hollow cathode condition and erosion parametres jet engineering. Issue 3(131). Jet thrusters and energy devices, Moscow, NIITP, 1991, p 108.

22. Moskaliov B.J. Hollow cathode discharge. M., Energy, 1969, p 184.

23. Dugev Y.A., Mitrophanov N.K., Starcev E.A., Shkolnik S.M., Yeurgev V.Y. Physical research of arc hollow cathode work. Preprint Ioffe Ph.T.I., N 58, 1978, p 57.

24. Buksht F.Y., Ribakov A.B., Yaigev V.Y. High-current arc cathode theory. Preprint. Ioffe Ph.T.I., N 789, S, 1982, p 60.

25. Zchukov M.F., Kozlov N.P., Pustogarov A.V. etc.Electrode processes in arc discharges. Novosibirsk, Science, 1982, p 157.

26. Dugev Y.A., Zimin A.M., Hvesuk V.I. Thermoemission cathodes. In. "Plasma accelerators and ion injectors". M., Nauka, 1984, p 200-217.

27. Drawin H.W., Z.Phys., 146, 295, 1956.

28. Gericke W.E., Z.Astrophys. 53, 68, 1964.

29. McNab J.R., Lindley B.C., Advances in Magnetohydrodynamics, Pergamon Press, N 4, 1963, pp. 27-46.

30. Gusinov M.A., Gerardo J.B., Verdeyen J.T., Phys. Rev., 149, 91, 1966.

31. Indraham J.C., Brown S.C., Phys. Rev. 138, A 1015, 1965.

32. Griem H.C., Plasma Spectroscopy, N.Y., 1964.

33. Meve R., De Vries R.F., Journ. Nucl. Energy, 6, 591, 1964.

34. Zehukov M.F., Koroteev A.S., Urukov B.A. Applied dynamics of thermal plasma. "Nauka", Novosibirsk, 1975.

35. Zehukov M.F., Anshakov A.S., Zasipkin I.M. et al. Arcjet generators with interelectrode inlets. "Nauka", Novosibirsk, 1981.